Master's thesis

NTNU
Norwegian University of Science and Technology
Faculty of Information Technology and Electrical Engineering
Department of Electric Power Engineering

Trygve Helseth

Effect of SF_6-alternative gas on the dielectric breakdown strength in load break switches

Master's thesis in Energy and Environmental Engineering
Supervisor: Associate professor Frank Mauseth
June 2019

NTNU
Norwegian University of Science and Technology

Trygve Helseth

Effect of SF_6-alternative gas on the dielectric breakdown strength in load break switches

Master's thesis in Energy and Environmental Engineering
Supervisor: Associate professor Frank Mauseth
June 2019

Norwegian University of Science and Technology
Faculty of Information Technology and Electrical Engineering
Department of Electric Power Engineering

NTNU
Norwegian University of
Science and Technology

Acknowledgements

I would like to thank my supervisors, associate professor Frank Mauseth and Dr. Nina Sasaki Støa-Aanensen, for their support and the opportunity to conduct my thesis work in this very interesting field of study.

Furthermore, I owe a debt of gratitude to SINTEF scientists Erik Roger Jonsson and Hans Kristian Hygen Meyer for their invaluable help in setting up the dynamic and static experiments.

A special thanks also go to the technical staff at both NTNU and SINTEF for their help with procuring and fabricating components for the experiments.

Trygve Helseth, Trondheim, June 2019

Abstract

Static dielectric testing was conducted on a pin & cup style contact pair. Gap distances of 6 mm and 10 mm, pressures of 1 bar and 1.3 bar, and gas compositions of technical air and a 7.5% AirPlus mixture were tested. An increase in gap distance from 6 mm to 10 mm resulted in a 30.87% or more increase in the $U_{16\%}$ breakdown voltage for all the tested configurations. For constant distance and a pressure increase from 1 bar to 1.3 bar, the resulting increase in the $U_{16\%}$ breakdown voltage was 23.60% or higher for all cases. The effect of AirPlus gas when compared to technical air yielded an increase in the $U_{16\%}$ breakdown voltage of 55% or more for all configurations.

Testing was carried out to investigate the relationship between static and dynamic breakdown voltage for a contact pair in atmospheric air. No general relationship was found.

Sammendrag

Det moderne kraftnettet inneholder stadig fler fornybare energikilder. Dette er svært gunstig for klimaavtrykket til samfunnets elektriske energiforbruk, men det gir også noen nye utfordringer. Overgangen til fornybare energikilder krever et mer fleksibelt og kontrollerbart strømnett. Den nøyaktige topologien til neste generasjons distribusjonsnett er fortsatt ubestemt, og ikke innenfor denne oppgavens omfang, men det vil mest sannsynlig inneholde en utbredt bruk lastbrytere. På steder der det allerede er begrenset plass, vil størrelsen på lastbryterne, og generelt for alle elkraftkomponenter, spille en stor rolle. For å oppnå kompakte løsninger har kraftindustrien siden 1970-tallet vært avhengig av bruk av svovelheksafluorid-gass (SF_6). SF_6-gass har omtrent tre ganger den dielektriske holdfastheten som atmosfærisk luft, dette gjør det mulig å produsere mye mindre utstyr for samme belastningsevne. Utmerkede termiske egenskaper gjør også SF6 til en ideell gass for bruk i brytere. Men dagens utbredte miljøfokus har kastet lys over problemene knyttet til bruken av SF_6-gass i elektrisk utstyr. På grunn av et globalt oppvarmingspotensial (GWP) på 22800 ganger CO_2, er alternative løsninger til bruk av SF_6 svært attraktive. Alternative gasser som tilbyr lignende egenskaper som SF_6, men uten den høye GWP, har kommet til markedet de siste årene. Industriselskaper som ABB, Siemens, og 3M tilbyr alle alternative gasser.

I denne masteroppgaven ble den statiske dielektriske holdfastheten til ABBs AirPlus-gass testet på et generisk "pin & cup" kontaktpar. Flere forskjellige parametere ble undersøkt. En økning i luftgap fra 6 mm til 10 mm førte til en økning i $U_{16\%}$ holdfastspenningen på 30,87% eller mer for alle oppsettene. For konstant avstand og en trykkøkning fra 1 bar til 1,3 bar var den resulterende økningen i $U_{16\%}$ holdfastspenningen 23,60% eller høyere for alle tilfeller. Effekten av AirPlus gass sammenlignet med teknsik luft ga en økning i $U_{16\%}$ holdfastspenningen på 55% eller mer for alle konfigurasjoner. Disse resultatene indikerer at AirPlus kan være en viktig faktor i utviklingen av kommende generasjons kompakte lastbrytere

Eksperimenter ble også utført for å utforske sammenhengen mellom statisk og dynamisk holdfasthet i atmosfærisk luft. Det ble ikke funnet en tydelig og generell sammenheng mellom de to i testene utført under denne oppgaven.

Contents

1 Introduction

The modern power grid steadily incorporates more renewable and intermittent power sources. This is highly beneficial for the overall climate footprint of society's electrical energy use, but it also poses some new challenges. The transition towards renewable energy sources requires a more flexible and controllable power grid. The exact topology of the next generation distribution network is still undecided, and not within the scope of this thesis, but it will by all accounts include an outspread use of Load-Break Switches (LBS). In places where space is already at a premium, the size the of LBSs, and all power grid equipment in general, will play a big role. To achieve compact solutions the power industry has since the 1970s relied on the use of Sulfur Hexafluoride (SF6) gas. SF6 gas has about three times the dielectric strength of air, this makes it possible to create much smaller equipment for the same voltage rating and pressure. Excellent thermal properties also make SF6 an ideal gas to utilize in switchgear. However, the present day widespread environmental focus has shed light on the problems associated with the use of SF6 gas in electrical equipment. Due to a global warming potential (GWP) of 22800 times CO2, alternative solutions to the use of SF6 are highly attractive. Alternative gases that offer similar attributes as SF6, but without the high GWP, have come to market in recent years. Industry giants like ABB, Siemens, and 3M all offer alternative gases.

Figure 1: AirPlus insulated 24 kV load break switch [1]

In this master thesis the static dielectric withstand voltage of ABB's AirPlus gas will be tested on a generic tulip plug contact pair (pin & cup). Results from these tests will be compared to tests of the same contact pair in technical air, and the effectiveness of the gas will be deducted.

Static dielectric testing is a relatively straightforward procedure, but in the real-world application of Load Break Switches the dynamic characteristics of the dielectric withstand voltage are of a much higher importance than the static characteristics. Dynamic dielectric testing is a more complex routine, requiring more equipment and setup time. Consequently, it is of interest to gain insight into how well static dielectric testing predicts dynamic behavior, as this could decrease time and cost spent in early development of switchgear design. Therefore, dynamic making tests of a contact pair will be conducted in atmospheric air. Results from this will be compared to the static testing carried out on the same contact pair during the specialization project.

This thesis will present the underlying theory, computational results where it is applicable, and the experimental results obtained.

2 Theory

The theory presented in this section covers physical phenomena used to describe different aspects of the dielectric breakdown, information regarding gas characteristics, and the underlying theory for some of the tools used in the analysis.

The following theory is compiled from [2, 3, 4]

2.1 Load Break Switches

Load break switches (LBS) are an integral part of the modern power network. They are used for interrupting currents below or equal the rated load current. In a power system the choice of LBS rating will reflect the maximum continuous current the network is rated for. The need to only interrupt load current is one of the facets of an LBS that significantly differs from a circuit breaker, as the circuit breaker need to be able to interrupt all currents, including short circuit currents. Closing of the switch represent the highest stresses for a load break switch. The reason for this is that closing may occur under fault conditions, meaning that the switch may be subjected to short circuit current during the making operation. Most of the commercially available LBS utilize either SF_6 or air as the interrupting medium. Compared to larger SF_6 circuit breakers, the pressure used in SF_6 load break switches is relatively low, often in the area between 1 and 1.5 bar. The switches using SF_6 will in general be more compact than an air-insulated switch of equal rating, but also more expensive. The use of an LBS in conjunction with a high voltage fuse may in some cases replace the function of a circuit breaker, and in turn reduce cost when compared to the cost of a regular circuit breaker.

2.2 Townsend avalanche

The Townsend avalanche theory describes a phenomenon that occurs when a gaseous media is subjected to an electric field. In the electric a field a free primary electron can be released due to some outside energy. This energy can be cosmic radiation, heat, or high local fields. The primary electron will move around in the gas and collide with the gas molecules. Because of the mass difference between the electron and the molecules, the electron will not lose significant energy during these collisions. When two bodies maintain their energy after a collision it is known as an elastic collision. While colliding with the molecules the primary electron is accelerated by the electric field towards the anode. At a certain point the electron will, due to its increased speed, have enough energy to ionize a molecule. When this energy is reached, the electron can collide with a molecule and in turn ionize the molecule. This ionizing collision generates additional electrons. These electrons are subjected to the same forces as the primary electron and can ionize new molecules, and in turn es-

tablish a chain reaction. This chain reaction will leave a channel of ionized gas which can facilitate a discharge, and consequently an electric breakdown.

The Townsend breakdown criterion is given by equation 2.1. It describes the current at the anode as a function of the gap distance, d. I_0 is the saturation current. The first Townsend ionization coefficient, α, is defined as the number of electron or positive ions produced per unit length. The second Townsend ionization coefficient, γ, describes the likelihood of production of secondary electrons.

$$\frac{I}{I_0} = \frac{e^{\alpha d}}{1 - \gamma(e^{\alpha d} - 1)} \tag{2.1}$$

2.3 Streamer mechanism

In the decades after the publication of the Townsend avalanche theory, experimental results proved that it often failed to predict the breakdown point for gaseous media with sufficient accuracy. This led to a new proposed theory on electric breakdown called the Streamer Mechanism.

If the electron avalanche, theorized by Townsend, reaches a critical size, an enhanced field is formed at the head of the avalanche. This increases the number of ionizing collisions and recombination. The recombination emits photons that can photoionize the gas and generate electrons for more avalanches close to the original electron avalanche's head. The superposition of these avalanches generates a conductive streamer. The formation of this streamer causes electric breakdown faster than the original Townsend avalanche theory predicts.

$$\int_{\Gamma} \alpha_{eff} dx = ln(N_{cr)} \tag{2.2}$$

Equation 2.2 describes the streamer breakdown criterion. The coefficient labeled α_{eff} describes the combined effect of the two Townsend ionization coefficients. Γ denotes the theorized streamer path. N_{cr} represents the critical number of electrons needed for a streamer discharge. α_{eff} is different depending on the field strength at that point in the streamer path. For this reason the calculation of α_{eff} differs depending on which range of field strength the point lies in. Equation 2.3 shows the equation for air in the range $12.36mm * bar < \mathbf{E}/p < 21kV/mm * bar$. A python [5] script is utilized to calculate the inception voltage based on the coefficient equations given in Petcharaks doctor dissertation [3]. The minimum background field required for stable streamer propagation in air is $0.54kV/mm$.

Within the scope of this project, the dielectric breakdown in gases can be sufficiently described by the Townsend avalanche, and the streamer mechanism.

$$\frac{\alpha_{eff}}{p} = C_1 * \frac{\mathbf{E}}{p} - A_1 \tag{2.3}$$

where:

$C_1 = 22.3591/kV$
$A_1 = 180.1711/mm * bar$

2.4 Streamer propagation

The streamer path is a subject heavily discussed in the literature. It has generally been said that the streamer propagates along field lines, but more recent studies suggest that the streamer is not so bound to field lines as previously thought [6, 7]. Advanced streamer line modeling is however outside of the scope of this thesis, and the simplified assumption that the streamer propagates along field lines will be employed.

2.5 Stochastic nature of dielectric breakdown

From the theory presented in the previous subsections it is established that the initial electron is created due some unpredictable mechanisms. This means that measurement taken under seemingly exact similar conditions could yield different results. There is an element of randomness to the breakdown process and the associated voltages that a breakdown occurs at.

2.6 Inhomogeneity

The electric field between two surfaces (eg. contacts) will vary depending on the geometry of said surfaces. For two plane and parallel surfaces (plane – plane configuration) the electric field between them will be close to homogenous (uniform), meaning that the electric field strength at any two given points in the space between the surfaces will be close to equal.

Most other two surface geometries will display characteristics of inhomogeneous fields (non-uniform fields). An inhomogeneous electric field is characterized by having a field strength that varies spatially between the surfaces.

There are no clearly defined measures for degree of inhomogeneity, but it is common to use eq. 2.4 as a simple measure. In this thesis the degree of inhomogeneity will be defined using eq. 2.4 on the simulated streamer. Meaning that the inhomogeneity of the contact pair will be the average field strength along the streamline divided by the max field strength along the streamline.

$$E_{inhomogeneity} = \frac{\overline{E}}{E_{max}} \tag{2.4}$$

2.7 Electron affinity

The theory of Townsend avalanches highlights the importance of the electron – gas molecule interaction. More specifically the attachment of electrons to gas molecules. The electron and gas molecule will have a summed energy before the attachment, and a combined energy after the attachment. The difference in these two energy levels are due to energy released during the attachment process, either as a photon or kinetic energy, and is denominated as electron affinity. Equation 2.5 describes the attachment process. Electron affinity can also be defined as the energy spent to attach a free electron to a neutral molecule. A highly electron affine gas will thus yield a higher dielectric strength.

$$X + e^{-1} = X^{-1} + E_{ea} \tag{2.5}$$

where:

X $=$ Molecule
E_{ea} $=$ Electron affinity

Gases with a high electron affinity are often composed of electronegative atoms. Due to this, highly electron affine gases have often been referred to as “electronegative gases” within the field of high voltage engineering, this is only partly correct as the isomeric structure of the molecule plays an important role in the degree of electron affinity. [2]

2.8 Other gas parameters

It is however not only the electron affinity of a gas that dictates whether the gas is suited as an insulating gas. Due to the nature of switchgear installations and handling, the insulating gas should be non-toxic, chemically stable, non-corrosive, and non-flammable. SF_6 ticks all the boxes of a great insulating gas, until global warming potential (GWP) is to be taken into account.

Table 1 shows some properties of SF_6 and a selection of alternative gases.

Insulating gas	Sulphurhexa-fluoride SF_6	Fluoro ketone (C5K) $C_5F_{10}O$	Trifluoroiodo-methane CF_3I	Hydrofluoro-olefin HFO1234zeE	Hydrochloro-fluoroolefin HCFO1233zd	Fluoro-nitrile C_4F_7N
Boiling point *) Sublimation point	-64 °C *)	+ 26.5 °C	-22.5 °C	-19 °C	+ 18.3 °C	-4.7 °C
GWP (CO_2: 1)	22,800	1	0.4	6	7	2,100
Ozone depletion potential	0	0	very low	0	very low	0
Flammability	no	no	no	no	no	no
Toxicity LC50 4h/rat (ppm)		>20,000	160,000 mutagene	>207,000	120,000	<15,000
Dielectric strength (LI) at -15 °C		85 % of SF_6 (air as a carrier gas)	120 % of SF_6	100 % of SF_6	90 % of SF_6 (air as a carrier gas)	120 % of SF_6 (air as a carrier gas)

Table 1: Property comparison between different insulating gases. ABB's AirPlus gas uses Fluoroketone (C5K) as its main component.[2]

2.9 Carrier gas

As switchgear installations are often subject to the environment, the insulating gas must be able to operate in the temperature range expected in the place of installation. For SF_6 this is not a problem, as the gas has a boiling point of -64 C. For other gases this poses a significant problem. The alternative gas Flouroketone (C5K) has a boiling point of +26.5 C and would therefore in most of northern Europe remain liquid, and only function on exceedingly hot summer days. To remedy this problem a carrier gas is mixed with the Flouroketone gas to lower the boiling point to satisfactory level. Nitrogen (N_2), Carbondioxide (CO_2), and technical air are common carrier gases. The addition of a carrier gas decreases the dielectric field strength to a certain degree, but the resulting gas mixture still performs satisfactorily. This technique, the addition of a carrier gas, is also used in some SF_6 installations, but in this case the object is not to lower the boiling point, but simply to decrease the amount of SF_6 gas used. Figure 2 shows the dielectric strength of SF_6 as a function of the amount of carrier gas added, here N_2 and CF_6. Figure 2 also shows that resulting dielectric strength does not necessarily change linearly with the amount of SF_6 present.

2.10 Paschen's law

Switches utilizing other insulating gas than atmospheric air need to be sealed. This increases the complexity of the component, but also gives to opportunity to pressurize the switchgear. The relationship between pressure and required voltage for dielectric breakdown (ignition voltage) is described by Paschen's law. Equation 2.6 shows Paschen's law in the analytical form. A Paschen curve is often used to visualize the law. The curve plots the ignition voltage as a function of the product of pressure and electrode distance, pd. Figure 3 shows the Paschen curve for some gases.

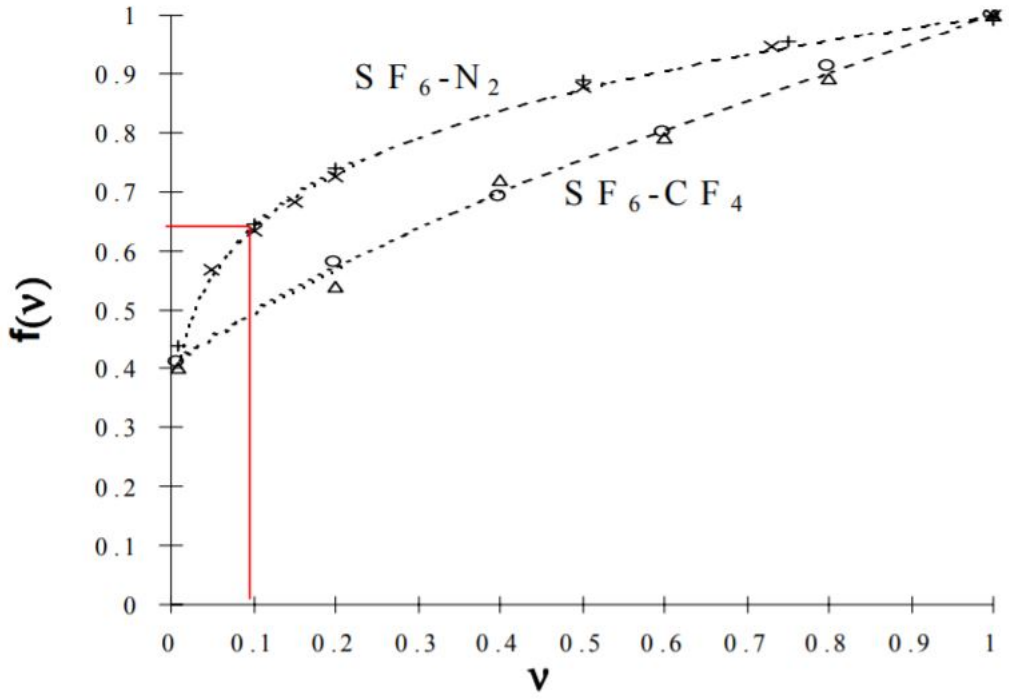

Figure 2: Normalised dielectric strength f(v) of SF_6 mixtures with nitrogen and CF4 as a function of the SF_6 volume concentration v [8]

It is observed that an increasing pd value will first decrease the ignition voltage until a minimum (Paschen minimum), then the ignition voltage will rise. As pd is the product between pressure and distance, a constant distance will yield the same ignition voltage characteristics for an increasing pressure, and vice versa. The Paschen minimum for air is 7.3 $bar * \mu m$. In switchgear application it is only rational to focus on pressures above and including atmospheric pressure. This means that at atmospheric air pressure, the distance the Paschen minimum is reached is 7.3 μm. It is expected that a breakdown will occur at distances much larger than that, therefore only the curve formed by pd values larger than the Paschen minimum is of value within the context of this work. With this "simplification" it can be said that for a constant electrode distance, the value of the ignition voltage will increase with increasing pressure. This holds true for all gases and pressures mentioned in the paper.

$$V_{bd} = \frac{B * pd}{ln\frac{A*pd}{ln(1+\frac{1}{\gamma}}} \tag{2.6}$$

where:

A, B = Constants
γ = Surface ionization coefficient

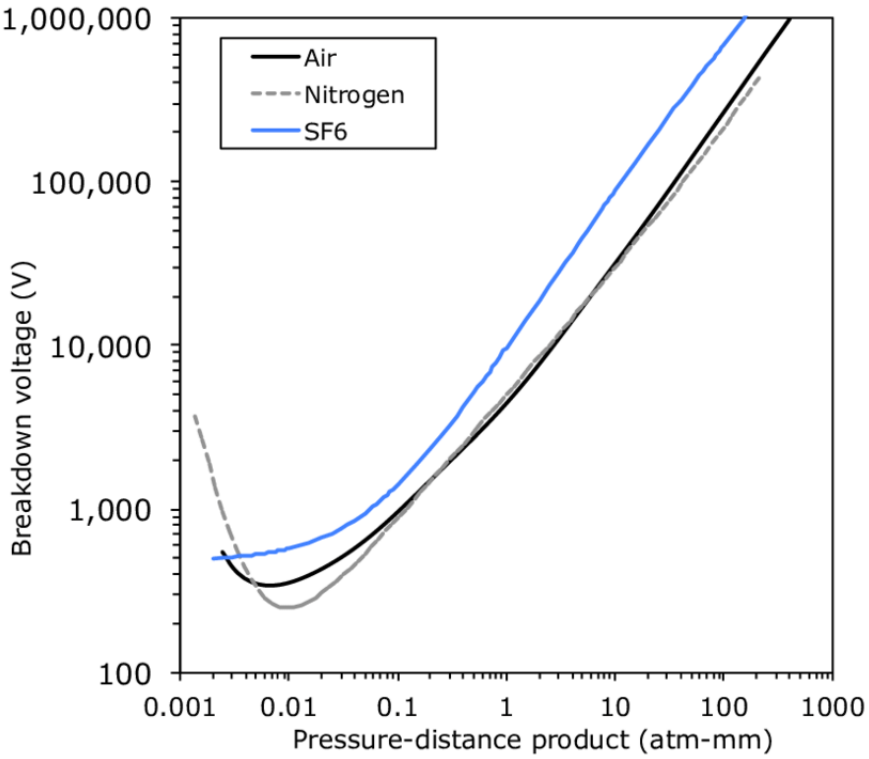

Figure 3: Paschen curves for SF_6, Air, and Nitrogen. [9]

2.11 Finite element method

Due to the complexity of the problems encountered in modern engineering, numerical methods are often employed to find adequate solutions. Finite element method (FEM) is one of the methods that sees widespread use. The FEM technique seeks to obtain approximate solutions to abstract calculus equations. A problem may be represented as a space with different domains. The domains have governing equations which describes how a certain phenomenon behaves within this domain. Governing equations can describe heat transfer, electric field etc. Along the edges of the domain there is a boundary condition that governs the value at that point. With the governing equation and boundary condition, one can find the values inside the domain through differential equations. It is however often quite difficult to obtain these values directly from the resulting differential equation due to the geometry of the domain. To remedy this, FEM divides the domain into smaller regions, called elements. The shape of the elements are simple geometries like triangles or quadrilaterals for two-dimensional domains, and tetra-, penta-, or hexahedra in three-dimensional domains. The system of these adjacent and non-overlapping elements is most often referred to as a mesh. With the domain meshed, it is possible to transform the governing equations into algebraic equations,

in this case called element equations. The element equations are much easier to solve, for both humans and computers, than differential equations that usually make up the governing equations. It is important to note that this transformation is at its core an approximation. It is now possible to evaluate the element equations, and the resulting values are combined into a new, much larger, set of equations. This set is called the system equations. At this point, the boundary conditions are introduced to the system equations, and the necessary adjustments are made to fulfill them. The resulting system equations are then solved. To ease interpretation, the results are post-processed, and displayed in tabular, graphical or other suitable forms.

Modern FEM software like COMSOL, OperaFEA, and Flux makes it easy to harness the power of the finite element method.

2.12 Regression analysis

To establish a trend in a dataset a regression analysis can be employed. A common form of regression analysis is the least square method. The least square method seeks to obtain a line that minimizes the sum of the hypothetical squares created between the line and the data points.

To perform a simple evaluation on how well the obtained line fits the data points the *coefficient of determination,* R^2, is often used. R^2 is, in its most general way, defined in 2.7. SS_{res} is here the sum of the squares obtained with the fitted line, and SS_{tot} is the sum of squares when the line is just the overall mean of the dataset. From the equation it is easily observed that the value of R^2 must lie between 0 and 1 depending on how well the line fits. A value close to 1 signifies a good fit.

$$R^2 = 1 - \frac{SS_{res}}{SS_{tot}} \tag{2.7}$$

2.13 Percentile

For a given dataset the percentile is the value which a certain percentage of the observations fall below. The 25% percentile (commonly referred to as the first quartile) is the value that 25% of the observations fall below. In breakdown testing it is common to employ the 16% percentile when presenting the results [10]. The 16% breakdown voltage percentile is denoted by $U_{16\%}$.

3 Computational setup

The inception voltage of a certain geometry in a medium can be calculated using a combination of finite element method and calculus.
The electric field between the contact pair is calculated using the finite element method (FEM). There are several programs that can be used for these calculations, and in this project the COMSOL software package was used [11]. The choice of COMSOL, as opposed to the other programs, was made because of previous experience with the software.

The COMSOL software package supplied by NTNU comes with the AC/DC module. This module simplifies the setup required by the user. In this project the contact pair is assumed to be axisymmetric, this cuts down the computational time required to do the calculations. Figure 4 shows the geometry used in COMSOL, the various boundary conditions, and the height parameter. In COMSOL the electric potential boundary condition is set to 24 kV.

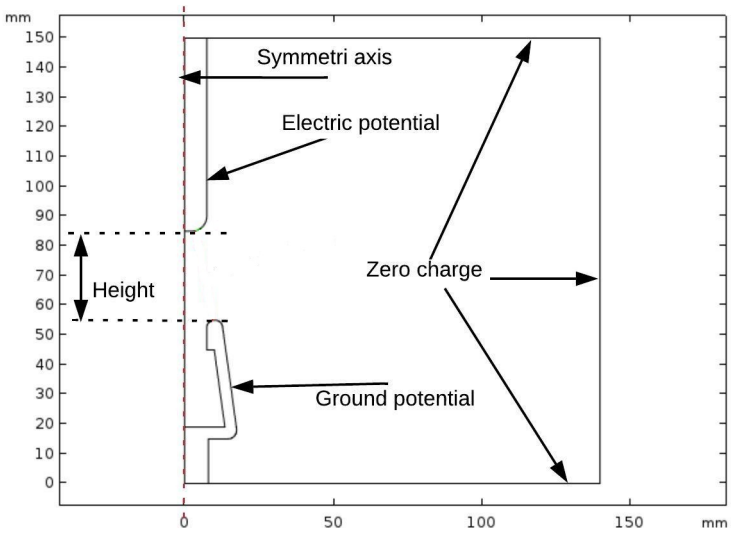

Figure 4: COMSOL model and boundary conditions

The electric field along several field lines are exported as a comma separated value file (CSV). To obtain the electric field for different heights a parametric sweep was used. This enabled the simulation of all the sought geometries without manual intervention, consequently greatly speeding up

the process.

Using the electric field calculated in COMSOL the inception voltage is calculated using a python script made by SINTEF researcher Hans Kristian Meyer . This script is based of Petcharaks doctor dissertation [3]. The script takes several field lines as input, calculates the inception voltage for all of them, and outputs the inception voltage for the field line with the lowest inception voltage. A brief theoretical background for this was presented in the streamer mechanism theory section. The script is given in appendix A.

4 Air and AirPlus static setup

The testing of the contact pair in Technical Air (denoted as Air onwards) and a 7.5% AirPlus gas mixture, with Air as the carrier gas, was conducted in the Subsea laboratory at SINTEF, Trondheim [12]. A new contact pair, figure 5, was designed and fabricated to fit in this setup. This lab and setup was also used during the thesis work of J.Glaus [10]. Care has been taken to emulate the setup and methodology of that thesis work, to facilitate a possible future comparison of the results.

4.1 Electric circuit

The electric circuit supplying the high voltage (AC) consists of a VARIAC, transformer, and water resistance, fig. 6. When connected to mains electricity the VARIAC is able to output a voltage ranging from 0 V to 230 V. The ramp time of VARIAC can be adjusted to suit different needs. The output from the VARIAC is connected to a 220:100 000 single-phase transformer. This yields a voltage capability of 0 V to 104 kV for the setup. To limit the current during breakdown a water resistance is placed between the HV side of the transformer and the 36 kV bushing on the gas vessel. This electric circuit is very similar to the circuit used during the "*Design and optimization of medium voltage switching contacts*" project [13].

4.2 Vessel and gas handling

To contain the AirPlus gas mixture and grant the ability to perform test at super-atmospheric pressure a gas vessel is utilized. The vessel has two viewing ports, one on each side, enabling photography. To increase or decrease the contact pair's gap length while still keeping the vessel closed a Rexroth linear actuator is used. Figure 7 shows the outside view of the vessel, and the contact pair within.

A DILO gas handling system, originally designed for handling of SF6 gas, is used for pulling a vacuum on the vessel in preparation for filling, and for the recovery of the AirPlus gas after testing. The filling procedure for both technical air and AirPlus starts with pulling a vacuum on the vessel. For technical air the next, and final, step is to pressurize the vessel to the desired pressure with technical air. The AirPlus filling is done by first adding the required amount of AirPlus gas to the vacuumized vessel, then filling to the final pressure with technical air.

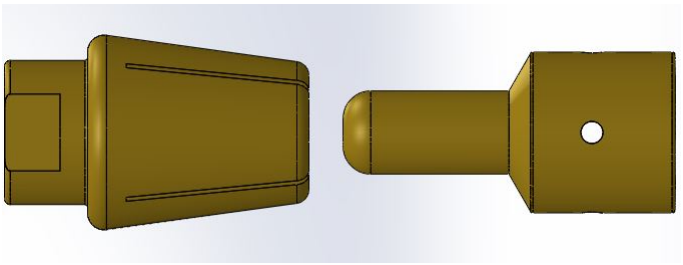

(a) Model view

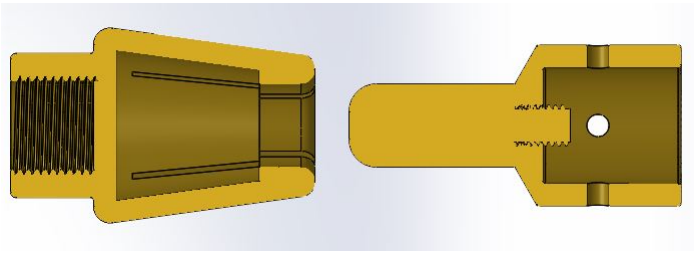

(b) Cutaway view

Figure 5: CAD model of the contact pair. The barrel of the pin contact is oversized to allow centering on the linear actuator via the use of setscrews.

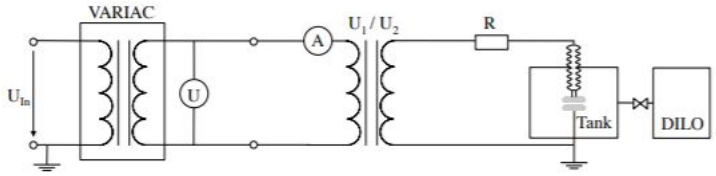

Figure 6: Schematic view of the setup used during testing [10]

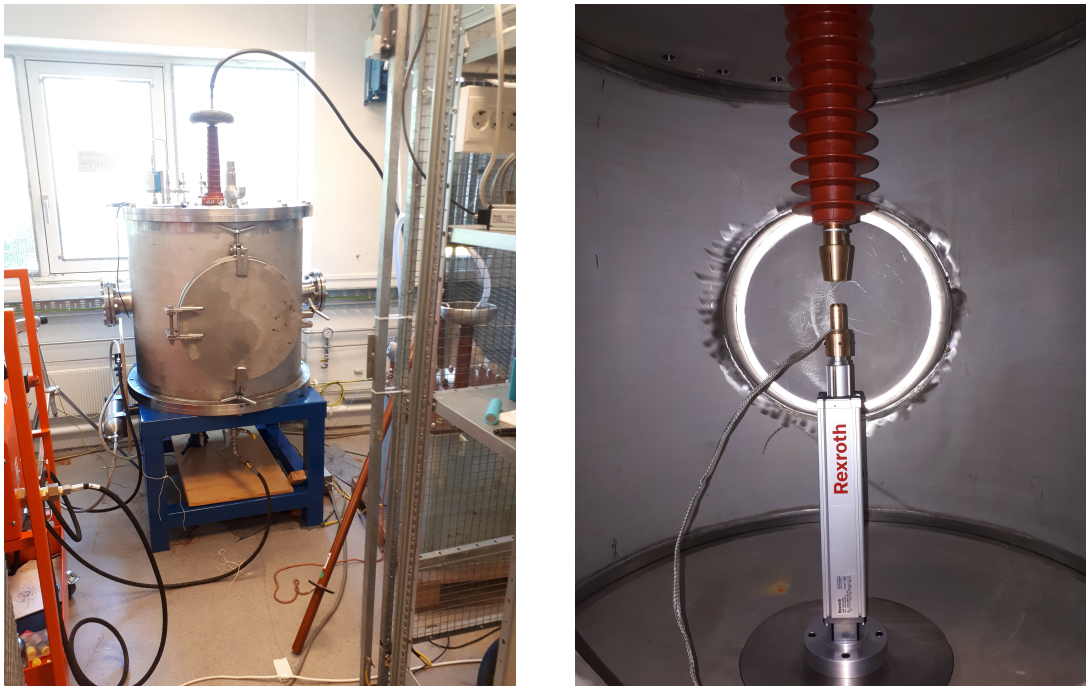

(a) (b)

Figure 7: (a): Outside view of the gas vessel. HV enters through the bushing at the top of the vessel. (b): View inside the vessel. The cup contact is attached to the HV side through the bushing. The pin contact is attached to the Rexroth linear actuator, and connected to ground via a braided metal cable.

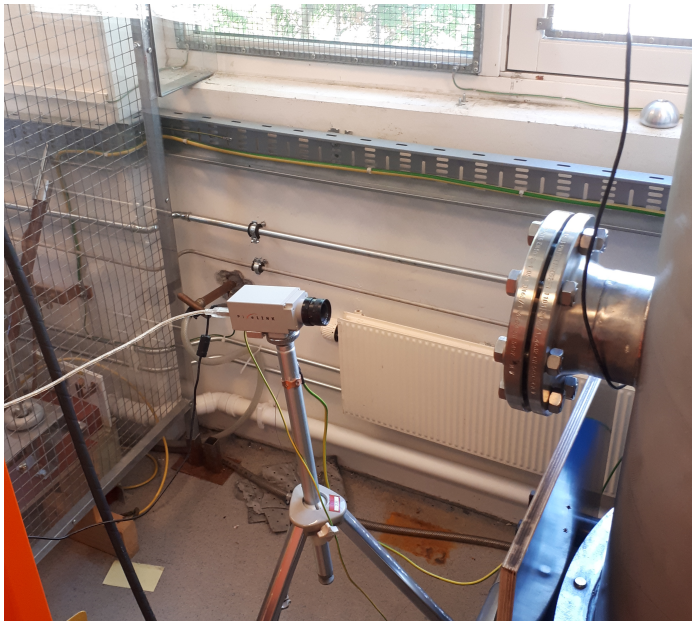

Figure 8: Camera setup outside the gas vessel

4.3 Measurement equipment

Voltage measurements are taken on the LV side of the transformer. These measurements are triggered by the current probe also connected to the LV side. The gas parameters, pressure, density, and temperature, are measured by a sensor inside the vessel.

4.4 Testing procedure

The procedure for conducting the experiment is deliberately mostly a copy of the procedure outlined in [10]. In appendix B the procedure used during this experiment is presented.

4.5 Videography

A Pixelink video camera and its associated software was used to capture the breakdown. Figure 8 shows the placement of the camera outside the vessel, looking in through the viewing port. A Matlab script was created to isolate the video frame at which the arc discharge happens. The script works by converting the video file to individual grayscale frames, and searching the images for high value pixels, meaning pixels that are very white. The images with high white values are then converted back to RGB images and outputted. This script can be a substantial time saver when compared to finding the frame of the arc discharge manually. The script is given in appendix F.

5 Dynamic testing setup

SOLIDWORKS [14] was used to design the contact pair. The design is based of common pin and cup designs. Figure 9a shows the finished design, figure 9b shows the cutaway view. The pin contact was made in two pieces to be replaceable either due to wear, or to experiment with different tip radiuses. In this experiment the exact same contact pair is used as in the static testing conducted during the "*Design and optimization of medium voltage switching contacts*" project [13]

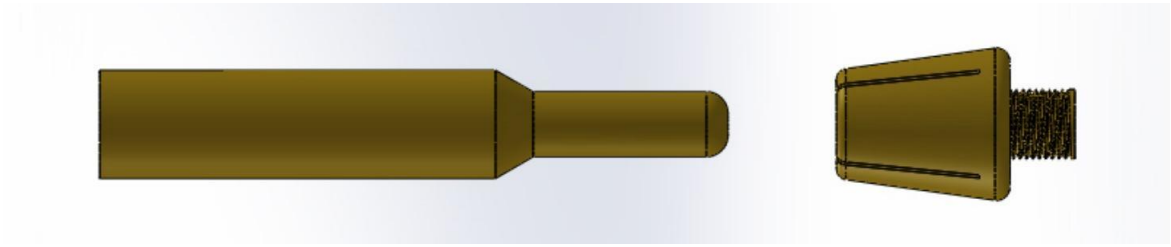

(a) Model view

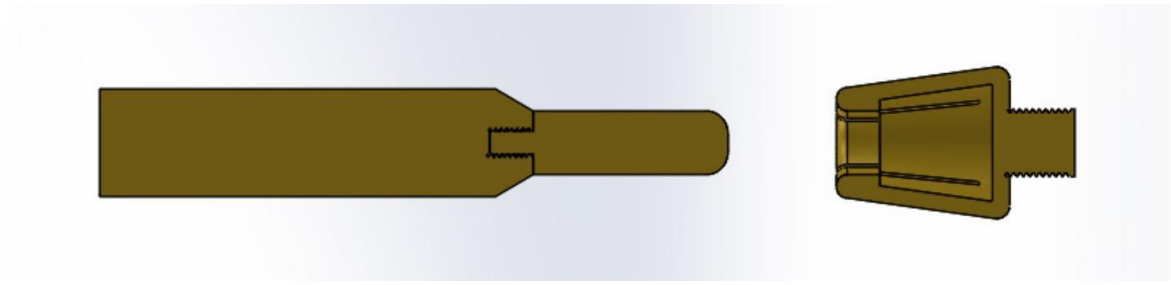

(b) Cutaway view

Figure 9: CAD model of the contact pair. (b) shows the two piece design of the plug contact and the interior design of the cup.

To determine the dynamic dielectric withstand voltage of the contact pair a setup with the capability of movement has to be used. The setup used in this project was designed and partially finished by a former PhD student at NTNU.

The major components of this setup are the mechanical assembly, HVDC source, capacitor, and the voltage divider.

5.1 Mechanical assembly

The mechanical assembly shwon in figure 10 is designed to move the pin contact and measure the position of said contact. Movement is achieved through the use of a spring. The pin contact is attached to a rod that can be pulled backwards by a block connected to a screw, this movement compresses the spring. At the full open position, the rod is held in place by an electromagnet, and the screw connected block can be withdrawn to its original position. The release of the electromagnet is controlled by fiber optics. Position is tracked by a linear resistance that is connected to the moving part of the assembly. The position sensor outputs a resistance, this resistance is converted to a voltage. Figure 11 shows the travel curve of the moving contact. The "overshoot" at the end of the movement is due to the rubber dampener placed at the end of the stroke. When the moving assembly hits this dampener the rubber compresses and absorbs some of the energy ensuring that the assembly is not damaged, the rubber then springs back.

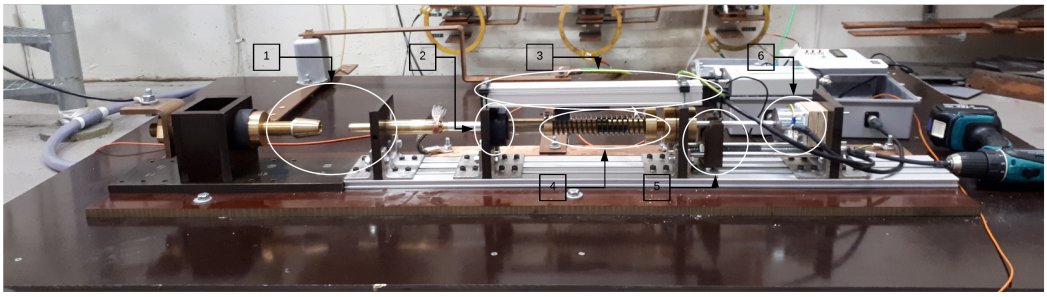

Figure 10: Mechanical assembly used for dynamic testing in the open position. 1: Contact pair, 2: Rubber dampener, 3: Position sensor, 4: Spring, 5: Screw connected block, 6: Electromagnet

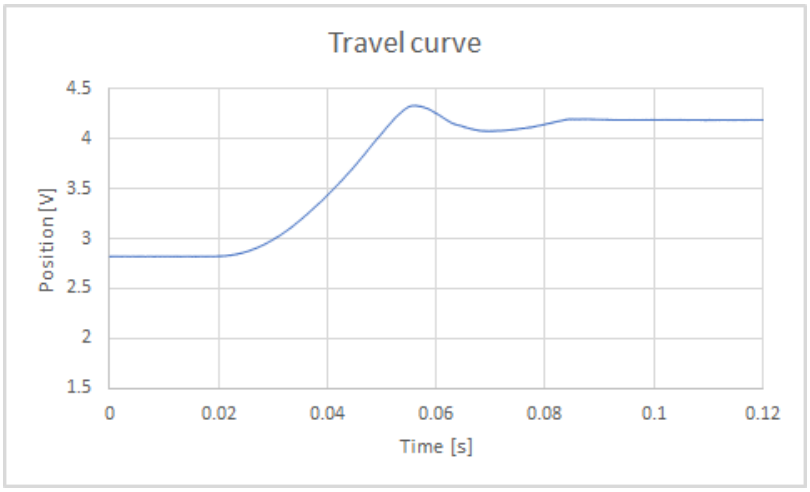

Figure 11: Travel curve of spring driven contact. Overshoot is caused by rubber dampener at the end of the assembly's stroke.

5.2 HVDC assembly

Figure 12 shows the HVDC assembly. HVDC is supplied by a SPELLMAN SL2000. This source is able to supply up to 30 kV DC voltage. The HVDC source is connected through a switch to the 100 nF capacitor. The two switches on the pallet are used to control the charging of the capacitor. Fiber optics are used to control the switches. Switch 1 in its default position connects the capacitor to ground (given that switch 2 also is in its default position). When switch 1 is engaged it connects the HVDC source to the capacitor. During testing it is desirable to disconnect the capacitor from the HVDC source, therefore switch 1 has to be disengaged right before the test. This also means that switch 2 should be engaged before this manoeuvre, as if switch 2 is left in its default position, the capacitor will then immediately discharge to ground through switch 2. When switch 2 is engaged it leaves the capacitor floating, ready to discharge through the contact pair. In practice the sequence in which the switches are switched are as follows:

1. Engage switch 2 (Remove direct grounding)
2. Engage switch 1 (Connect HVDC source to capacitor)
3. Turn on HVDC source, and charge capacitor (Done with fiber optics)
4. Disengage switch 1 (The capacitor is now floating)
5. Release contact (Done with fiber optics)
6. Turn off HVDC source
7. Disengage switch 2 (Reconnect ground)

The full order of operations that was employed during the experiment is given in appendix C.

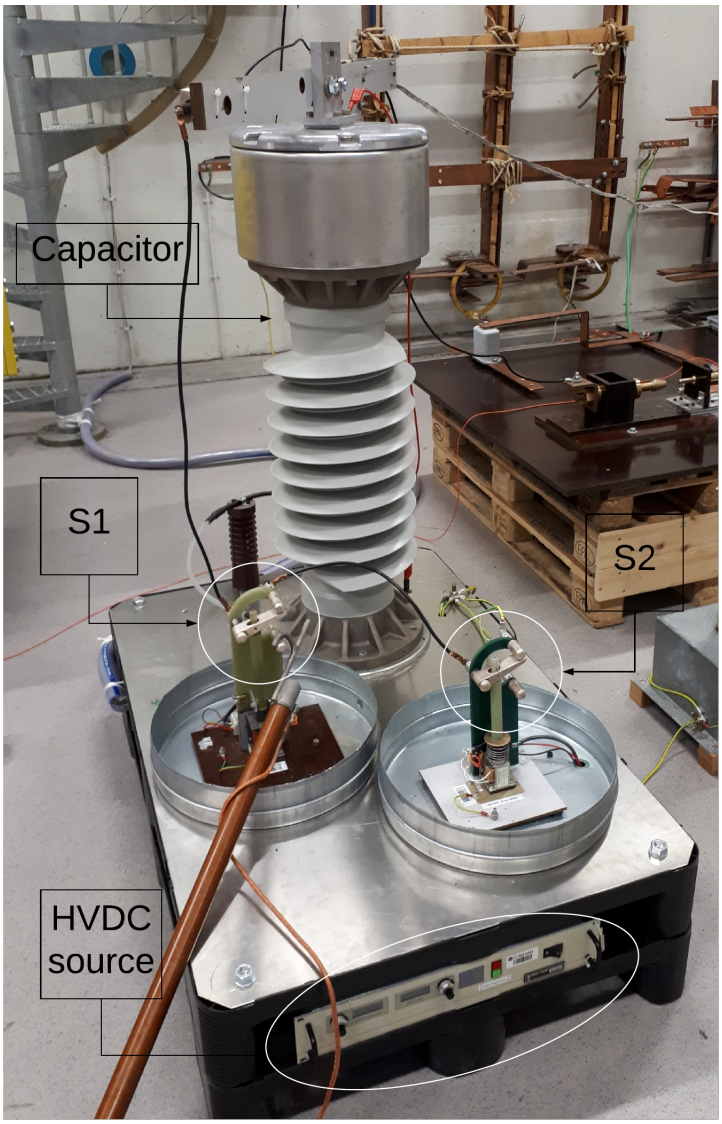

Figure 12: HVDC assembly consisting of source, capacitor, and switches. Note also the grounding rod on switch 1 used during setup and in between test to ensure safe working conditions.

5.3 Voltage divider

To measure the voltage at the time of dielectric breakdown a voltage divider is used. The voltage divider consists of a capacitive divider and a resistive divider connected in parallel. This results in a measuring system that has a low discharge rate, making measurements more repeatable. The

divider has a ratio of 10000:1, meaning that an input of 10 kV will result in 1 V at the output side of the voltage divider. For the HVDC source used in this experiment, this gives a output ranging from 0 V to 3 V. The division ratio is dictated by the input voltage range of the fiber optic links used in this experiment. In this case the fiber optic links used has a range of +/- 5 V.

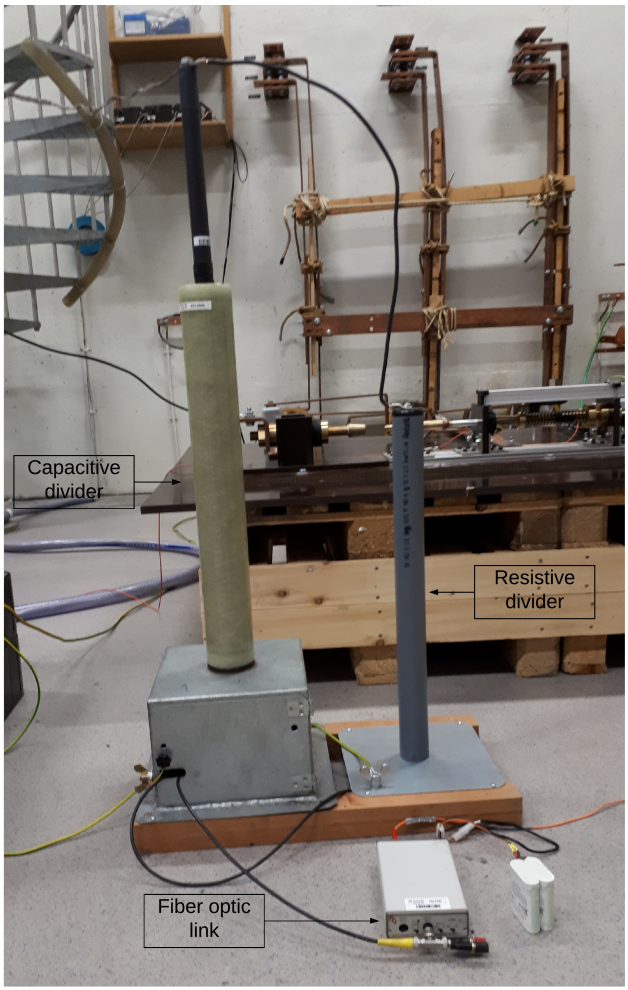

Figure 13: Resistive-capacitive voltage divider. Also shown is one of the fiber optic links used during testing.

5.4 Signal processing and Triggering

All signals to and from the test setup are done by fiber optics. The input to the setup are controlled from the lab control room. Output from the measurements (voltage and position) are converted from voltages to fibre optic signals with the use of a TTI fiber optic link. A computer software is

used to output a trigger sequence that releases the holding magnet on the mechanical assembly and starts the measurement capturing software. This will yield a measurement of both the voltage and position in volts. These voltage values are then post processed to give the actual voltage of the breakdown and the distance in mm.

5.5 Calibration

The position sensor outputs a voltage that changes depending on the position. For the purpose of this experiment the absolute position of the contacts is of importance, the voltage should therefore be converted into a length measurement. Voltage measurements were taken at different known distances, and the relationship between the voltage and distance was deduced.

Calibration of the fiber optic links was done by applying a known voltage on the input, and checking with the measured voltage shown in the capture software. These results are then used to establish a correction factor that can be applied to the experiment results.

6 Results

6.1 Computational

The results acquired from the simulation setup outlined in Chapter 3 are presented in this section. Figures 14 and 15 shows the graphical representation of the electric potential and electric field calculated by the FEM software. In the electric field representation the electric field lines are also presented. For visual clarity only 10 field lines are shown in figures 14(b) and 15(b), in the actual simulation 20 lines were used. These lines and their associated field strength along the line are used to calculate the inception voltage using the script presented in Chapter 3 and appendix A. The resulting inception voltages for Air and AirPlus in different configurations are given in table 2.

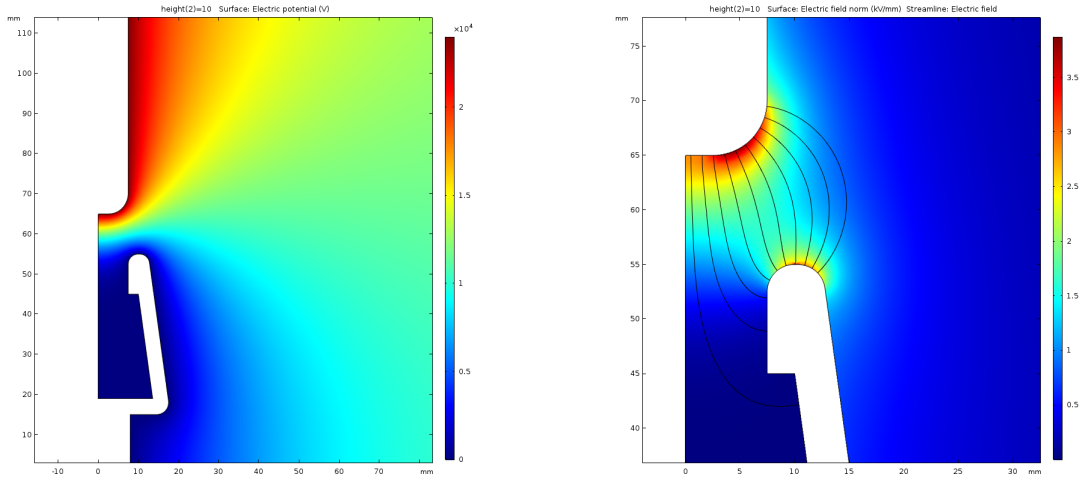

(a) Electric potential

(b) Electric field and streamlines

Figure 14: COMSOL plots for 10 mm with 24 kV applied voltage

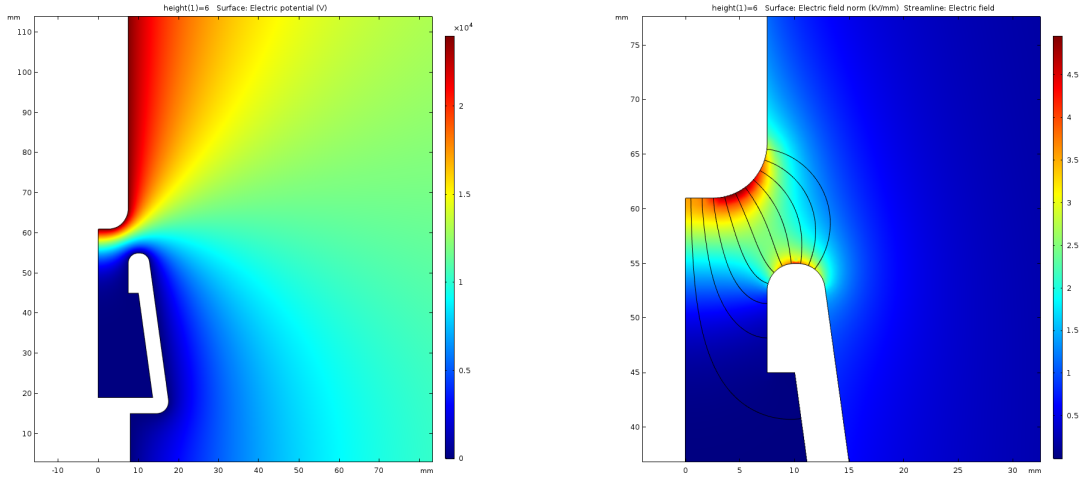

(a) Electric potential

(b) Electric field and streamlines

Figure 15: COMSOL plots for 6 mm with 24 kV applied voltage

	Air		AirPlus	
Pressure [bar] / Distance [mm]	1	1.3	1	1.3
6	22.73	28.15	34.44	43.51
10	29.21	36.19	44.18	55.78

Table 2: Calculated inception voltages in kV

6.1.1 Inhomogeneity factor

Using the electric field values from the dominant streamline the Inhomogeneity factor was calculated using eq.2.4. Table 3 gives the values for the two different gap distances.

Gap distance [mm]	Inhomogeneity factor
6	0.58
10	0.50

Table 3: Calculated inhomogeneity factors for 6 mm and 10 mm gap distances

6.2 Static AirPlus experiment

In this section the experimental results from the setup presented in Chapter 4 are given.
Eight different configurations were tested with 19 breakdown test each, resulting in a total of 152 breakdown experiments. Table 4 summarizes the $U_{16\%}$ breakdown voltages of the experiments.

	Air		AirPlus	
Pressure [bar] / Distance [mm]	1	1.3	1	1.3
6	21.93	28.31	35.51	43.89
10	29.70	37.05	46.57	57.65

Table 4: Experimental $U_{16\%}$ breakdown voltages in kV

6.2.1 Gap distance

Figure 16 shows the breakdown voltage as a function of the gap distance for four different configurations. The percentagewise increase in breakdown voltage when the gap length is increased is presented in table 5.

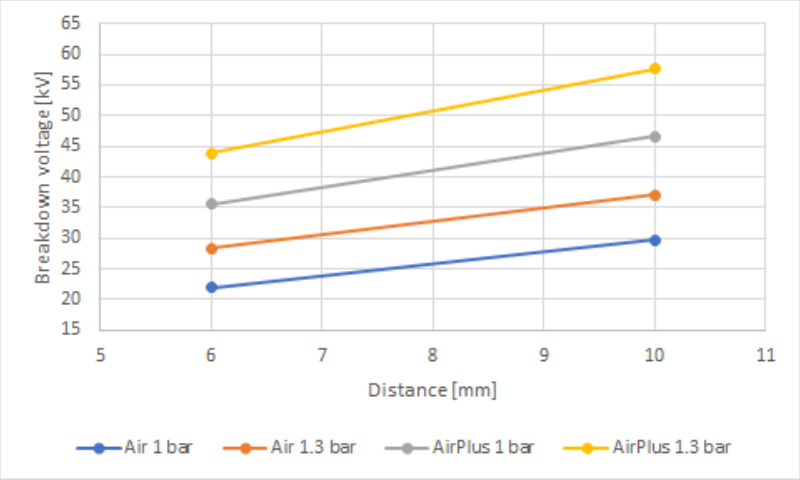

Figure 16: $U_{16\%}$ breakdown voltage for four configurations plotted as a function of the gap distance

Gas	Pressure [bar]	% increase in breakdown voltage
Air	1	35.34%
	1.3	30.87%
AirPlus	1	31.15%
	1.3	31.35%

Table 5: Percentagewise increase in $U_{16\%}$ breakdown voltage when increasing the gap distance from 6 mm to 10 mm

6.2.2 Pressure

The breakdown voltage as a function of pressure for four different configurations are presented in figure 17. Table 6 shows the percentagewise increase in breakdown voltage for an increase in pressure.

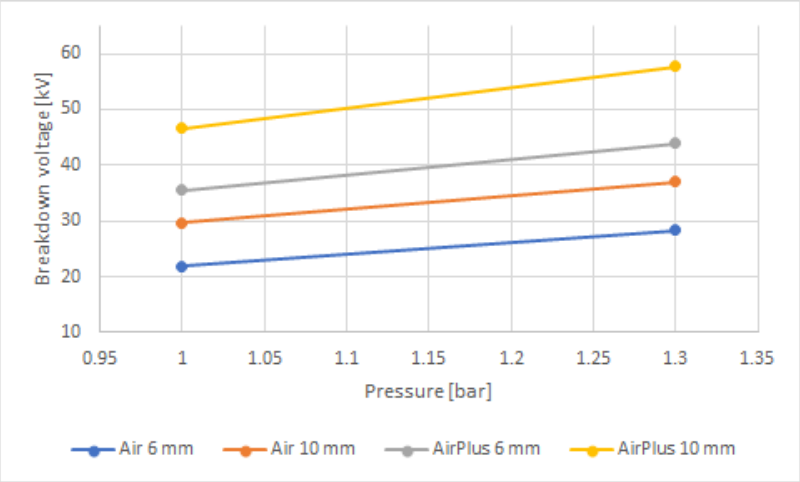

Figure 17: $U_{16\%}$ breakdown voltage for four configurations plotted as a function of the pressure

Gas	Distance [mm]	% increase in breakdown voltage
Air	6	29.09%
	10	24.75%
AirPlus	6	23.60%
	10	23.79%

Table 6: Percentagewise increase in $U_{16\%}$ breakdown voltage for an rise in pressure from 1 bar to 1.3 bar

6.2.3 Gas

Figure 18 shows the breakdown voltage of Air and AirPlus for different sets of parameters. The percentagewise increase in breakdown voltage when changing from Air to AirPlus is presented in table 7.

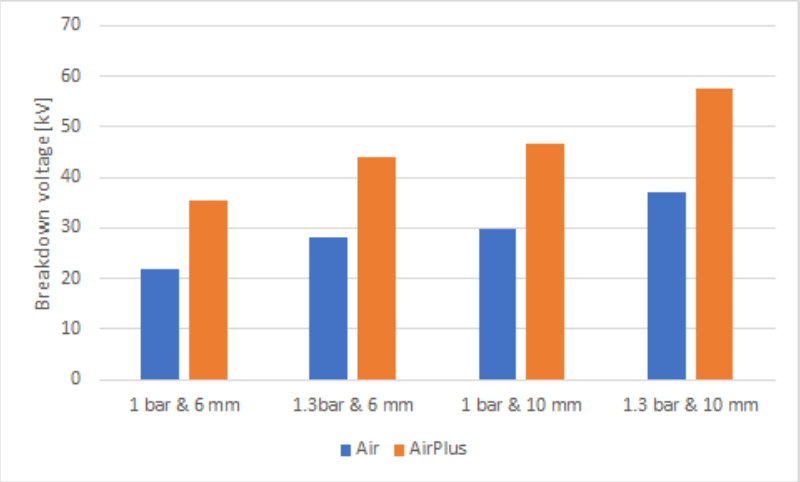

Figure 18: $U_{16\%}$ breakdown voltage of Air and AirPlus for different sets of parameters

Pressure [bar]	Distance [mm]	% increase in breakdown voltage
1	6	61.92%
	10	56.80%
1.3	6	55.03%
	10	55.60%

Table 7: Percentagewise increase in $U_{16\%}$ breakdown voltage when changing from Air to AirPlus

6.2.4 Photographs

Figures 19 and 20 shows five of the arc discharge photographs for each of the eight configurations. The full picture sets are given in Appendix G.

6.2.5 Comparison between simulations and experiments

The percentagewise difference between the experimental static setup and computational results are presented in table 8.

	Air		AirPlus	
Pressure [bar] / Distance [mm]	1	1.3	1	1.3
6	-3.52%	0.57%	3.11%	0.87%
10	1.68%	2.38%	5.41%	3.35%

Table 8: Percentagewise difference between the $U_{16\%}$ experimental breakdown voltages and the computational results. The percentage is calculated as the experimental value's difference from the computational

(a) Air
Distance = 6 mm Pressure = 1 bar

(b) Air
Distance = 10 mm Pressure = 1 bar

(c) Air
Distance = 6 mm Pressure = 1.3 bar

(d) Air
Distance = 10 mm Pressure = 1.3 bar

Figure 19: Arc discharge photos for the four Air setup configurations

(a) AirPlus
Distance = 6 mm Pressure = 1 bar

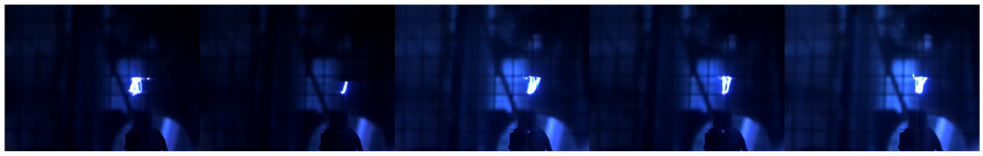

(b) AirPlus
Distance = 10 mm Pressure = 1 bar

(c) AirPlus
Distance = 6 mm Pressure = 1.3 bar

(d) AirPlus
Distance = 10 mm Pressure = 1.3 bar

Figure 20: Arc discharge photos for the four AirPlus setup configurations

6.3 Dynamic experiment

Using the setup specified in Chapter 5 a total of 45 breakdown experiments were conducted. Figure 21 shows the breakdown voltage graphed as a function of the distance where the breakdown occurred. A polynomial regression of the dataset is represented by the dotted line, and the equation of the line and R^2 value is given in the bottom right corner of the graph.

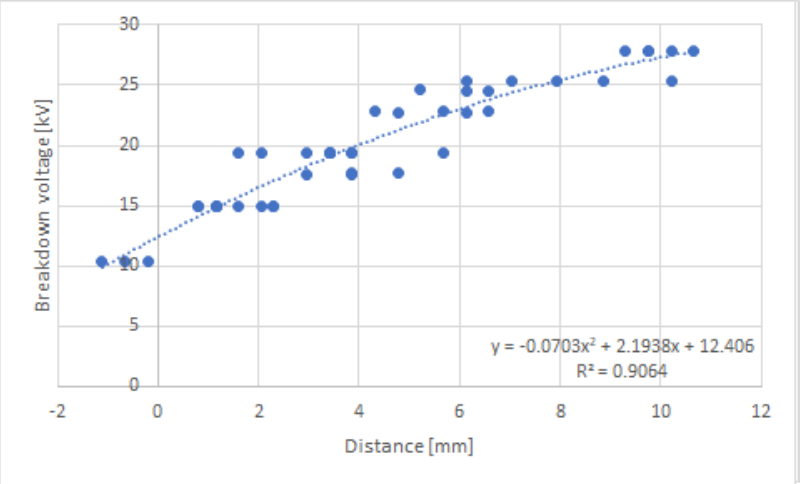

Figure 21: Dynamic testing breakdown voltage in atmospheric air as a function of distance. Dotted line represents the polynomial regression of the dataset. NOTE: Due to the coordinate system used during testing, where 0 distance is the 0 y-axis distance between the contacts, some distance measurements for lower voltages are negative. Refer to the *Height* parameter in figure 4 for a graphical representation of the distance coordinate system

6.3.1 Comparison between static and dynamic testing

In the "*Design and optimization of medium voltage switching contacts*" [13] static breakdown testing was conducted on the same contact pair as now tested dynamically. For a detailed description on how this static testing was carried out please refer to [13]. The polynomial regression of the data gathered in [13] is plotted alongside the the dynamic results from section 6.3 in figure 22. Figure 23 shows the difference in percent between the two experiments.

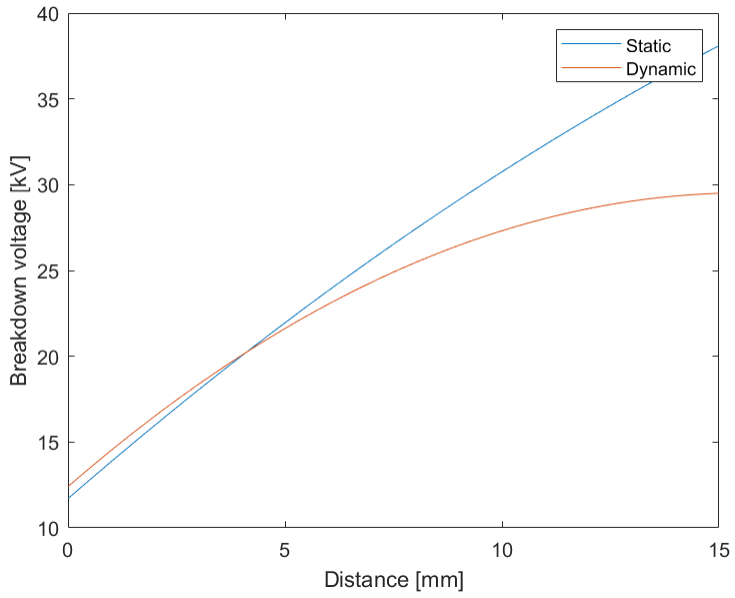

Figure 22: Polynomial regression curves of both static and dynamic experiments in atmospheric air

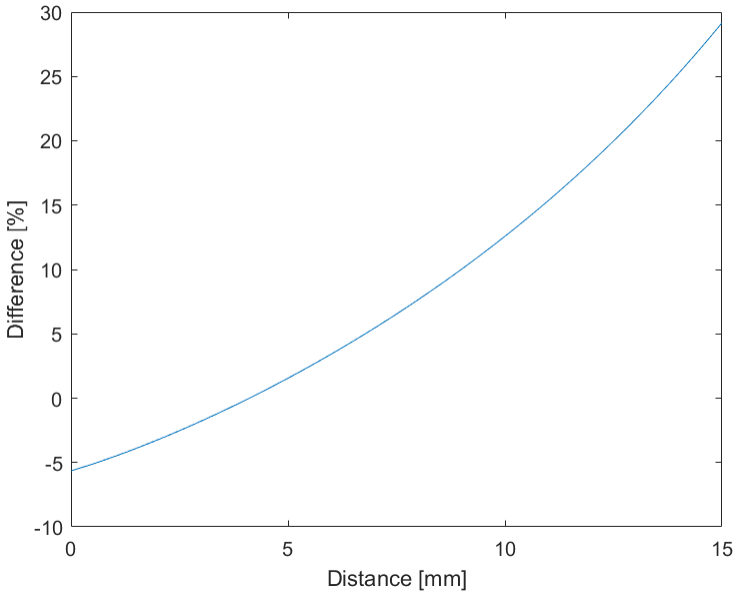

Figure 23: Percentagewise difference between the polynomial regression curves of the static and dynamic experimental testing in atmospheric air shown in figure 22

7 Discussion

The results obtained in Chapter 6 will in this section be discussed and analyzed.

7.1 Computational

7.1.1 Inhomogeneity Factor

It is important to note that the inhomogeneity factor is a purely calculated value based on the computational model. Experimental measurements of electric fields are outside the scope of this thesis.

Table 3 shows that the inhomogeneity factor decreases for an increased gap distance, in other words, the setup gets more inhomogeneous for larger gap distances. This is in line with established theory.

In this thesis the inhomogeneity factor is calculated on the basis of electric field values along the dominant streamline. An other way to calculate the factor is to base the average and max field values on a domain rather than a streamline. Figure 24 shows an example domain. This approach is difficult to implement for as complex geometries as the contact pair used in this thesis. The size and shape of the domain will cause great differences in the resulting inhomogenity factor. A very large domain will lead to very low average field value, and in turn very low inhomogenity factor. For these reasons the streamline approach has been preferred in this thesis, as it is less dependent on human choices.

7.2 Static setup

7.2.1 Gap distance and pressure

Table 5 and figure 16 clearly shows that the $U_{16\%}$ breakdown voltage increases with an increased gap distance for constant pressure. These results are in line with Paschen's law described in chapter 2. Table 6 and figure 17 shows that the same theory holds true for an increase in pressure with constant gap distance. In both the cases the one of the four results have a significantly higher percentagewise increase in the $U_{16\%}$ breakdown voltage. The common element in both these results is the measurement series for "*Air 6 mm 1 bar*".

The difference in percentagewise increase in breakdown voltage between the two cases, increased gap distance and increased pressure, are not of interest to directly compare as the factor of increase in the two cases are not the same.

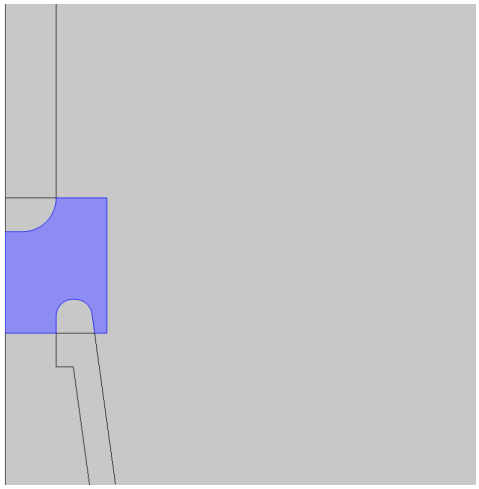

Figure 24: Example of a domain, highlighted in blue, that could be used for a domain based approach to inhomogeneity factor calculation

7.2.2 Gas

The effect of the AirPlus compared to Air for the contact pair is shown in table 7 and figure 18. All of the configurations boast an increase in the $U_{16\%}$ breakdown voltage of over 55% when the AirPlus gas mixture is used. This increase in breakdown voltage is as expected due to the fact that AirPlus contains an electron-affine fluoroketone. The effect of electron-affine components is described in section 2.7. Once again has the configuration containing the "*Air 6 mm 1 bar*" measurement series a significantly higher percentagewise increase in breakdown strength.

7.2.3 Photographs

The arc discharge photos presented in figures 19 and 20, and appendix G clearly shows that the experiments conducted in AirPlus produce a larger and more luminous arc than the Air experiments. However, the reason for this is by all accounts just a consequence of the increased breakdown voltage required for the AirPlus tests. This assumption is strengthened by the looking at the picture series for "*Air 10 mm 1.3 bar*" and "*AirPlus 6 mm 1.3 bar*", which both have similar $U_{16\%}$ breakdown voltage and in turn also similar luminosity.

A violent arc can cause issues in load break switches due to contact erosion. In the test setup used in this thesis there is only a very small current that is carried in the discharge arc, and as a result the arc has very low power and a low potential for causing erosion. Figure 25 shows the contact pair used during the static testing after all 152 breakdown experiments. The pair hardly show any wear, despite being made from brass. This would most likely be very different if the contact pair had been tested with a realistic amount of current. For this reason modern switch contacts often employ the more durable material *silver tungsten carbide* in arcing contacts [15].

Figure 25: Pin contact used for 152 breakdown test in the setup described in Chapter 4

7.2.4 Comparison between simulations and experiments

Table 8 presents the difference between the experimental values and computational values. All the differences fall within an acceptable margin of error. The reason for calling a difference value as high as 5 % acceptable is due to the, relatively, huge discrepancy between the CAD model contact pair used in the simulation and the actual physical contact pair fabricated and used during the experiment. This discrepancy could be reduced by using high precision CNC (Computer Numerical Control) fabrication machines and techniques. The precision of the height and contact pair's concentricity achieved in the setup will also contribute to the overall error.

With the exception of the "*Air 6 mm 1 bar*" configuration, all configurations have higher experimental breakdown voltages than the computational results. Ideally all simulations would be dead on, but it is generally considered that conservative simulations are the lesser of two evils when compared to simulations that yield very optimistic and, in the case of switchgear, potentially dangerous results.

7.2.5 "*Air 6 mm 1 bar*" measurement series

The "*Air 6 mm 1 bar*" measurement series has been an element is all the comparisons that have had a significant difference from the others. This could indicate that the configuration behaves significantly different when subjected to high voltage, which would be very interesting, or it could indicate some problems with the actual data gathered from the tests.

The actual measured gas parameters, listed in appendix D, shows that the pressure during the "*Air 6 mm 1 bar*" testing was a bit lower than the value used during simulation, and the other configu-

rations it has been compared against. When the simulation is run with a pressure of 0.995 bar, the calculated inception voltage is 0.42 % lower than with 1.000 bar. This could explain some of the difference, but not all.

Looking it the raw data supplied in appendix D, the "*Air 6 mm 1 bar*" measurement series does differ some from the other configurations. It has together with the "*Air 10 mm 1 bar*" measurement series the largest percentagewise spread in measurement values. In the case of the "*Air 10 mm 1 bar*" measurement series this spread is due to an outlier value, but in the "*Air 6 mm 1 bar*" measurement series there are no extreme outliers, just a gradual increase in breakdown voltage over the course of the testing. This could signify some trouble with the actual measurement series and data gathering.

7.3 Dynamic setup

One of the main goals of this thesis was to examine the relationship between the results of static and dynamic testing. Matching results or results that differ by a simple factor would mean that static testing could be used to make accurate predictions of the dynamic breakdown voltage. The results presented in section 6.3.1 does not indicate a relationship of this kind. Figure 22 shows that the two experiments correlate well at small gap distances, but from ∼6 mm and upwards the values drift apart. This could indicate that there is not a simple relationship between the two experiments, but could also be a manifestation of the differences between the experiments.

A large difference is the use of AC voltage in the static testing, and DC in the dynamic testing. This has most likely contributed to significant differences between the two datasets. The dynamic testing does not have data for voltage values over ∼30 kV due to the limitation of the HVDC source used during the experiment. This limits the number of data points in the dynamic dataset greatly. Testing at higher voltages could perhaps yield a smaller difference between the two tests.

8 Conclusion

The goal of this thesis was to investigate the effect of AirPlus gas on the dielctric breakdown strength of a contact pair. A secondary objective was to examine the relationship between static and dynamic breakdown strength in atmospheric air.

In the static Air and AirPlus testing the effect of several different parameters were investigated. For the configurations used in this work, an increase in gap distance from 6 mm to 10 mm yielded an increase in the $U_{16\%}$ breakdown voltage of over 30.87% for all cases. For constant distance and a pressure increase from 1 bar to 1.3 bar, the resulting increase in the $U_{16\%}$ breakdown voltage was 23.60% or higher for all cases. The effect of AirPlus gas when compared to Air yielded an increase in the $U_{16\%}$ breakdown voltage of 55% or more for all configurations. Most of the experimental values were in line with the values predicted by the computational model.

These results indicate that AirPlus could be an important factor in the development of the coming generation compact load break switches. It is worth noticing that the effect of AirPlus gas decreases with increasing inhomogeneity [10], and as a result more time and resources should be put into optimizing the contact geometry to obtain a more homogeneous electric field distribution.

A clear general relationship between the static and dynamic breakdown strength in atmospheric air was not found during the work conducted in this thesis. The values correlated well at low gap distances, but quickly drifted apart for increased when the gap distance grew beyond 6 mm. As the two setups used for static and dynamic testing differ so much, it is difficult to dismiss the possibility of a relationship based on these results.

9 Further work

There is certain value and potential in further studies of AirPlus and other SF_6 alternatives. The static AirPlus setup used in this work is of high quality and should be applicable for future research projects.

- The main focus should be to acquire more data for different parameters, and in turn produce a more comprehensive study on the effect of AirPlus gas on complex geometries.

- AirPlus switchgear, and other alternative gas switchgear, could probably benefit from a design optimization of the contact pair for use with the new gas. Emphasis should be put on achieving a more homogeneous electric field, while still satisfying all the other attributes that are demanded of a contact pair.

- A possible relationship between static and dynamic breakdown voltage should be investigated further. Care should be placed on designing setups that are similar, so that the two results can be easily compared.

Bibliography

[1] ABB. Gas-insulated ring main unit safering airplus. https://new.abb.com/medium-voltage/switchgear/gas-insulated-switchgear/iec-gis-rmu-for-secondary-distribution/iec-gas-insulated-ring-main-unit-safering-airplus. Accessed: 2019-05-09.

[2] Küchler, A. 2018. *High Voltage Engineering*. Springer Vieweg.

[3] Petcharaks, K. 1995. *Applicability of the streamer breakdown criterion to inhomogenous gas gaps*. Ph.D dissertation.

[4] Burnett, D. 1987. *Finite Element Analysis: From Concepts to Applications*. Addison-Wesley Longman, Incorporated.

[5] Rossum, G. Python. [Programming language]. URL: https://www.python.org/.

[6] Pedersen, A., Christen, T., Blaszczyk, A., & Boehme, H. October 2009. Streamer inception and propagation models for designing air insulated power devices. In *Proc. IEEE Conf. Electrical Insulation and Dielectric Phenomena*, 604–607.

[7] Nijdam, S., Takahashi, E., Teunissen, J., & Ebert, U. 2014. Streamer discharges can move perpendicularly to the electric field. *New Journal of Physics*, 16(10), 103038.

[8] Niemeyer, L. 05 2019. Cigre guide for sf6 gas mixtures. application and handling in electric power equipment.

[9] Babrauskas, V. 2013. Arc breakdown in air over very small gap distances. In *Proc. Interflam*, volume 2, 1489–2149.

[10] Glaus, J. 2019. *Breakdown Characteristics of AirPlus and Air in MV Applications*. Master thesis.

[11] COMSOL. Comsol multiphysics. [Software]. URL: https://www.comsol.com/.

[12] SINTEF. The subsea laboratory. https://www.sintef.no/en/all-laboratories/the-subsea-laboratory/. Accessed: 2019-05-21.

[13] Helseth, T. 2018. *Design and optimization of medium voltage switchingcontacts*. Specialization project.

[14] Dassault Systèmes. Solidworks. [Software]. URL: https://www.solidworks.com/.

[15] Mützel, T. & Kempf, B. October 2014. Silver tungsten carbide contacts fork circuit breaker applications. In *Proc. IEEE 60th Holm Conf. Electrical Contacts (Holm)*, 1–7.

A Inception voltage script

```
#!/usr/bin/env python3
# -*- coding: utf-8 -*-


"""
Created on Fri Jan  5 17:00:44 2018

@author: hanskrme / pap

This script calculates inception voltages along a single line in air from
COMSOL simulations using fit functions from Petcharaks PhD thesis, 1995. It
takes either a field line with electric field strength in kV/mm and distance in
x and y directions in mm from a 2D simulation or a cut line in 2D or 3D with
field strength in kV/mm and distance along the line (arc length) in mm. Also,
the applied voltage must be given.

Two classes are implemented, one for field lines (FieldLine2D()) and one for
cut lines (CutLine()). To instantiate a new class, type

new = CutLine(filename, delimiter, applied voltage)

or

new = FieldLine2D(filename, delimiter, applied voltage)

depending on the type. Example:

new = CutLine('edge.csv', ',', 10)

new = FieldLine2D('field_line2D.csv', ',', 35)

To view inception voltage, print the class attribute u_i:
print(new.u_i)

Run this script to see an example.


Also, the script estimates breakdown voltage based on propagation distance
U = E_st*d + U_0, where E_st = 0.54 kV / mm, U_0 = 23.7 kV

To view propagation voltage, print the class attribute Uprop:
print(new.Uprop)

"""

import numpy as np
import abc
import glob
import os

class Line:
    __metaclass__ = abc.ABCMeta

    @abc.abstractmethod
    def get_values(self, line):
        return
```

1

```
def __init__(self, file, delim, voltage):
    return

def import_file(self, file, delim):
    line = np.loadtxt(file, delimiter=delim)


def get_inception(self, line):
    if self.medium == 'air':
        STREAMER_CONSTANT = 9.15  # for ionization integral
    elif self.medium == 'air+':
        STREAMER_CONSTANT = 12.9
    elif self.medium == 'sf6':
        STREAMER_CONSTANT = 10.15

    U = self.voltage  # kV, applied voltage
    P = self.pressure # pressure
    k = 0.01  # voltage scaling factor
    STEP_SIZE = 0.001
    C = 0  # counter
    u_i = 0  # Inception voltage
    while C < STREAMER_CONSTANT:


        #  Scale field
        field = self.E*k
        #  FIND ALPHA
        alpha = np.zeros(len(field))
        for i in range(len(field)):
            if self.medium =='air':
                if field[i]/P > 14:
                    alpha[i] = (1175*np.exp(-28.38*field[i] / P)) * P
                if field[i]/P > 7.943 and field[i]/P <= 14:
                    alpha[i] = (16.7766*(field[i]/P)-80.006)*P
                if field[i]/P >= 2.588 and field[i]/P <= 7.943:
                    alpha[i] = (1.6053*(field[i]/P-2.165)**2-0.2873)*P
            elif self.medium == 'air+':
                if field[i] / P > 10 and field[i] / P <= 19.2:  # Nina suggestion
                    alpha[i] = (19.452 * field[i] / P - 118.48)*P
                if field[i] / P >= 5.53 and field[i] / P <= 10: #Nina suggestion
                    alpha[i] = (17.418*field[i] / P -97.46)*P

            elif self.medium == 'sf6':
                if field[i] / P > 30:
                    alpha[i] = (2078 * np.exp(-43.3 / field[i] / P)) * P
                if field[i] / P >= 12.36 and field[i] / P < 30:
                    alpha[i] = (22.359 * field[i] / P - 180.171) * P
                if field[i] / P >= 8.9246 and field[i] / P < 12.36:
                    alpha[i] = (27.9 * (field[i] / P - 8.2946)) * P

            else:
                print('Du må velge riktig medium. air,ari+ eller sf6')

        C = np.trapz(alpha, self.dist)
        u_i = U*k
        k = k+STEP_SIZE
    return u_i
```

2

```
    def get_propagation(self):
        return 0.54*self.l + 23.7


class FieldLine2D(Line):
    def __init__(self, line, voltage, pressure, medium):
        self.voltage = voltage
        self.pressure = pressure
        self.medium = medium
        self.get_values(line)
        self.u_i = self.get_inception(line)
        self.Uprop = self.get_propagation()
        #self.import_file(file, delim)

        return

    def get_values(self, line):
        line = np.stack(line)
        #line = line[np.argsort(-line[:, 1])]
        self.x = line[:, 0]
        self.y = line[:, 1]
        self.E = line[:, 3]
        self.get_distance()

    def get_distance(self):
        self.dist = np.zeros(len(self.x))
        dl = np.zeros(len(self.x))
        for i in range(0, len(self.x)-1):
            dl[i] = np.sqrt((self.x[i+1] - self.x[i])**2 +
                            (self.y[i+1] - self.y[i])**2)
            self.dist[i+1] = self.dist[i]+dl[i]
        self.l = self.dist[len(self.dist)-1]


class CutLine(Line):
    def __init__(self, file, delim, voltage):
        self.voltage = voltage
        self.import_file(file, delim)

    def get_values(self, line):
        self.dist = line[:, 0]
        self.l = self.dist[len(self.dist) - 1]
        self.E = line[:, 1]


class Bundle:
    def __init__(self, file, delim):
        f_line = []
        self.f_lines = []
        lines = np.loadtxt(file, delimiter=delim)
        i = 0
        for line in lines:
            if int(line[2]) == i:
                f_line.append(line)
            else:
                self.f_lines.append(f_line)
```

3

```
                f_line = []
                f_line.append(line)
                i += 1
        self.f_lines.append(f_line)


        #self.import_file(file,',')


if __name__ == '__main__':

    # new = CutLine('cut_line_3D.csv', ',', 10)
    # print('Example: Inception voltage cut line: ')
    # print(new.u_i)
    # print('Example: Breakdown voltage cut line: ')
    # print(new.Uprop)

    list_of_files = glob.glob('./*.csv')
    media = ['air', 'air+', 'sf6']
    pressure = [1, 1.3]
    p = pressure[1]
    bundle = True

    if os.path.isfile('inception.txt'):
        os.rename('inception.txt', 'inception.txt.bak')

    with open('inception.txt', 'a') as out_file:

        for p in pressure:
            for file in list_of_files:
                air = []
                airplus = []
                sf6 = []

                bundle = Bundle(file, ',')
                for field_line in bundle.f_lines:
                    air.append(FieldLine2D(field_line, 24, p, 'air').u_i)
                    airplus.append(FieldLine2D(field_line, 24, p, 'air+').u_i)
                    sf6.append(FieldLine2D(field_line, 24, p, 'sf6').u_i)


                print(file[2:] + ': ' +str(p)+', '+ str(min(air))+', '+str(min(airplus))+', '+ str(
                out_file.write(file[2:] + ',' + str(p) + ',' + str(min(air)) + ',' + str(min(airplu

            #print(new.u_i)
        #print('Example: Breakdown voltage field line: ')
        #print(new.Uprop)

    out_file.close()
```

B Testing procedure static setup

From [10].

- Preparation:
  - Contacts
    - Install the contact pair and clean them with isopropanol
  - Gas
    - Vacuumize gas vessel
    - Fill gas vessel with
      - Technical Air
      - AirPlus (fill first ketones and then add technical air)
    - Switch on warning lamp due to high pressure
-
  - Gas measurements
    - Measure pressure in the tank
    - Measure temperature in the tank
    - Measure gas density in the tank
- Breakdown test:
  - Remove grounding
  - Apply 10 kV for 3 min before first breakdown
  - Increase voltage until breakdown
  - Apply the 10 kV again
  - Start clock for the 3 min interval
  - Increase voltage until breakdown
  - ...
  - Repeat this until 19 breakdown tests are carried out
- After Experiment:
  - Switch off voltage
  - Ground experiment
  - Measure again pressure, temperature and density of gas

C Order of operations dynamic testing

Inside the lab:

- Control all ground connections
- Remove the safety wire (RED) that short circuits the capacitor
- Disable the fire alarm with the timer.
    - Located in the corner
- Connect batteries to the different sender boxes, and position sensor
- Switch on the fiber optic links
    - Always on 1 MΩ and 5 V
- Turn on HVDC source
- Remove grounding rod

Inside the control room:

- If the computers are not already on, turn them on
- The program to use on the left computer is called “Hoved_PCI_03”
    - First screen: press measure
    - Adjust timing
    - Press “start måling” to start measurement. This will not take a measurement but wait for a trigger signal.
- On the right computer the program is called “Time sequence controller”
    - The current preset is found in the file “2018_forløp_V2” which is located in the folder “Time sequence” on the desktop
    - Note that CH1 must be active to perform triggering from this program.
- Turn on the fiber optic trigger box
- If turned off, turn on the power supply
    - · Do not change the voltage level!

To test:

- Press “Inn” on the interlock box
- On the HVDC source controller box the following switch sequence is used:
    - Note that all the switches must be pushed all the way over to function.

1. “Jording” On

2. “Ladebryter” On
3. “HV on/off” On
4. Use “Motor up” or “Motor down” to adjust the voltage
5. Start measurement on left computer, “Start måling”
6. Switch off the “ladebryter” on the controller box and press “Start sequence” on the right computer.
    - This two step sequence has to happen relatively fast

- Turn off “HV on/off” and “Jording”
- To save the measurement, press “Lagre måledate” on the left computer
- Press “ut” on the interlock control box
- Open the door, ensure that the HVDC source has reached zero or 0.1 on the display
- Use the earthing rod to ground the capacitor and the switch terminal that is directly connected to the HVDC source.

D Raw data static setup

Distance [mm]	Peak [kV]
6	19.41
6	19.54
6	22.88
6	22.5
6	22.88
6	21.86
6	22.5
6	23.14
6	22.63
6	22.24
6	23.14
6	23.66
6	23.14
6	23.53
6	24.56
6	24.56
6	23.4
6	24.56
6	24.68
Pressure [bar]	0.995
Density [$\frac{kg}{m^3}$]	1.19
Temperature [°C]	21.06

Distance [mm]	Peak [kV]
10	30.21
10	34.2
10	29.57
10	31.76
10	30.08
10	31.63
10	29.7
10	30.73
10	30.73
10	37.03
10	30.21
10	31.24
10	31.11
10	29.96
10	29.7
10	28.67
10	31.5
10	30.73
10	33.94
Pressure [bar]	0.999
Density [$\frac{kg}{m^3}$]	1.20
Temperature [°C]	22.76

Table 9: Air 1 bar

Distance [mm]	Peak [kV]
6	29.7
6	29.96
6	29.44
6	29.96
6	30.86
6	31.37
6	28.67
6	29.44
6	28.8
6	29.83
6	29.83
6	28.41
6	28.93
6	29.44
6	28.93
6	28.28
6	28.8
6	28.03
6	28.28
Pressure [bar]	1.298
Density [$\frac{kg}{m^3}$]	1.55
Temperature [°C]	21.42

Distance [mm]	Peak [kV]
10	37.16
10	39.86
10	40.63
10	38.96
10	40.76
10	40.24
10	40.24
10	40.76
10	43.07
10	41.4
10	39.73
10	38.06
10	38.06
10	37.03
10	37.03
10	37.03
10	38.31
10	42.81
10	41.53
Pressure [bar]	1,299
Density [$\frac{kg}{m^3}$]	1.55
Temperature [°C]	21.23

Table 10: Air 1.3 bar

Distance [mm]	Peak [kV]
6	36.26
6	36.38
6	35.87
6	36.51
6	36.9
6	35.61
6	36.38
6	36.77
6	36.64
6	36.26
6	33.81
6	36.38
6	35.74
6	35.48
6	35.36
6	35.87
6	35.87
6	36.51
6	36.13
Pressure [bar]	1.000
Density [$\frac{kg}{m^3}$]	1.93
Temperature [°C]	21.74

Distance [mm]	Peak [kV]
10	46.67
10	47.57
10	48.08
10	48.08
10	46.03
10	47.83
10	46.93
10	47.83
10	48.08
10	47.05
10	46.93
10	47.57
10	47.44
10	47.57
10	46.28
10	46.54
10	48.34
10	47.05
10	47.83
Pressure [bar]	1.001
Density [$\frac{kg}{m^3}$]	1.94
Temperature [°C]	21.58

Table 11: AirPlus 1 bar

Distance [mm]	Peak [kV]
6	45.77
6	46.41
6	46.15
6	46.15
6	46.8
6	45.77
6	45.13
6	46.8
6	46.28
6	46.03
6	43.58
6	45.77
6	46.28
6	45.25
6	40.5
6	46.41
6	45.25
6	43.58
6	45.13
Pressure [bar]	1.299
Density [$\frac{kg}{m^3}$]	2.50
Temperature [°C]	21.56

Distance [mm]	Peak [kV]
10	58.24
10	58.88
10	58.88
10	58.11
10	59.27
10	59.4
10	57.6
10	58.88
10	57.47
10	59.14
10	57.85
10	59.14
10	58.88
10	58.88
10	59.14
10	59.4
10	56.57
10	58.75
10	59.14
Pressure [bar]	1,300
Density [$\frac{kg}{m^3}$]	2.49
Temperature [°C]	21.93

Table 12: AirPlus 1.3 bar

E Raw data dynamic setup

Pos [mm]	U [kV]
4.77	22.71
6.13	22.71
4.32	22.81
5.68	22.81
6.58	22.81
8.85	25.34
10.20	25.34
6.13	25.34
7.94	25.34
7.04	25.34
10.66	27.78
10.20	27.78
9.75	27.78
9.30	27.78
9.75	27.78
3.42	19.40
3.42	19.40
2.96	19.40
1.61	19.40
3.87	19.40
2.06	19.40
3.42	19.40
5.68	19.40
3.87	19.40
3.42	19.40
5.23	24.68
6.13	24.58
6.58	24.48
-1.11	10.42
-0.21	10.42
-0.66	10.42
3.87	17.63
2.96	17.63
3.87	17.73
4.77	17.73
1.15	14.91
2.06	15.01
2.28	14.96
1.61	14.96
0.81	14.96
0.81	14.96
2.28	14.96
1.15	14.96
1.15	14.96
1.15	14.96

F Framespotting

```
% Framespotting v3
% by Trygve Helseth
% Matlab version R2019a
% Req: Image Processing Toolbox


clear all

folder = 'Name'; %Video folder
info = dir(fullfile(folder));
info([info.isdir]) = [];

nfiles = length(info);

newfolder= strcat(folder,'_photos');
mkdir (newfolder); %Make new folder for photos

for i = 1: nfiles

  filename = fullfile(folder, info(i).name);
  [filepath,name,ext] = fileparts(filename);


    Movie = VideoReader(filename); %Read videofile
    nframes = get(Movie, 'NumberOfFrames'); %Total number of frames in the video
    array = (1);
    clear Im
    clear Img
    counter=1;

    for k = 1 : nframes
        Frame = read(Movie, k);
        Frame=rgb2gray(Frame); %Convert to grayscale
        Diff=max(Frame,[],'all');
        if Diff > 250          %sets the "sensitivity". 255 is max white value.
            array(counter)=k;
            counter=counter + 1;
        end
    end

    lArray=length(array);

    if lArray == 1
        Img = (read(Movie,array(1)));
        sparkframe = array(1);

    else

        for j =1 : length(array)
            Im{j}=(read(Movie,array(j)));
        end
```

```
        montage(Im)
        x=input('Choose picture:');
        sparkframe=array(x);
        Img=(read(Movie,array(x)));
    end
        imshow(Img);
        y=input('Correct picture? yes=1, no=2 ');
        if y==1

        Img=(read(Movie,sparkframe));
        baseFileName=strcat(name,'.png');
        fullFileName= fullfile((newfolder), baseFileName);
        imwrite(Img,fullFileName);


        elseif y==2

            for nn = 1:nframes
                frames {nn}= (read(Movie,nn));
            end

            for mm= 1:(nframes/25)
                montage(frames, 'Indices', ((mm-1)*25+1):((mm-1)*25+25))
                z=input('Frame within selection? Yes=1, No=2 ');
                if z==1
                    picNum=input('Frame number?');
                    Img = read(Movie,((mm-1)*25+picNum+1));

                    imshow(Img);
                    baseFileName=strcat(name,'.png');
                    fullFileName= fullfile((newfolder), baseFileName);
                    imwrite(Img,fullFileName);
                    break
                end
            end
        end
end
```

```
Warning: Directory already exists.
```

Published with MATLAB® R2019a

G Arc discharge pictures

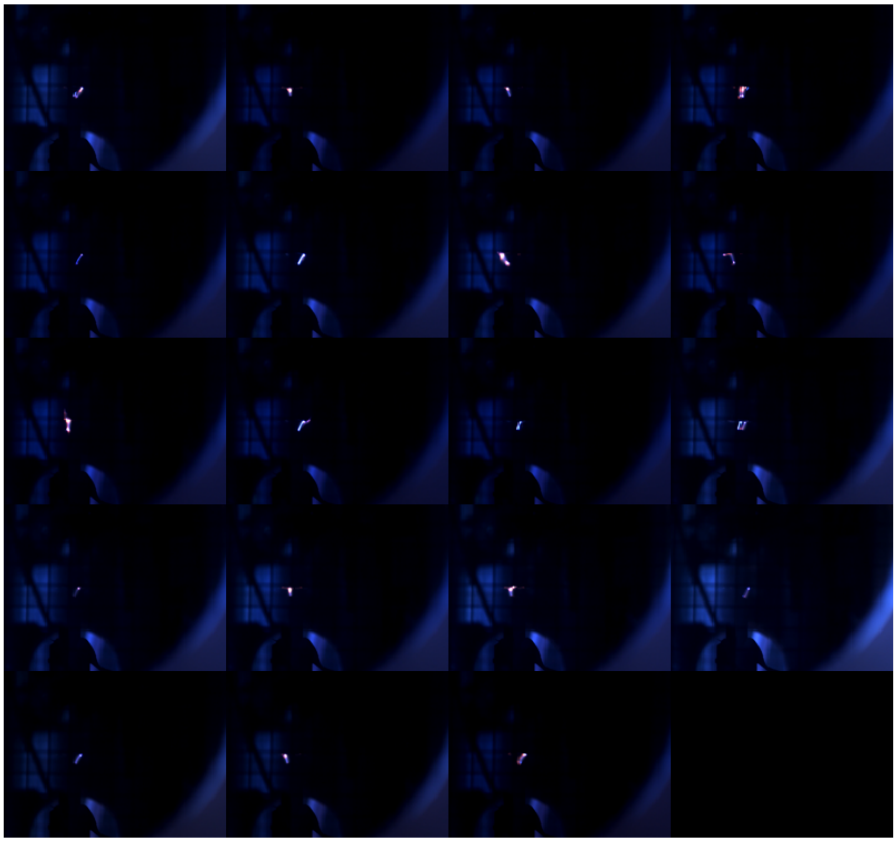

Figure 26: Air
Distance = 6 mm Pressure = 1 bar

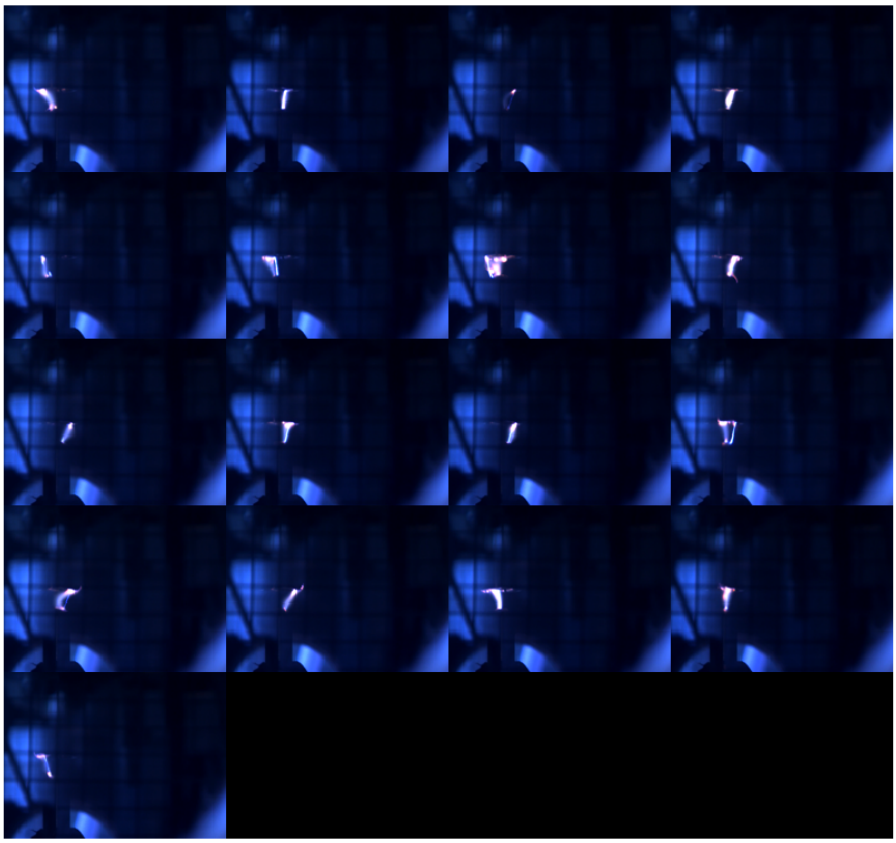

Figure 27: Air
Distance = 10 mm Pressure = 1 bar

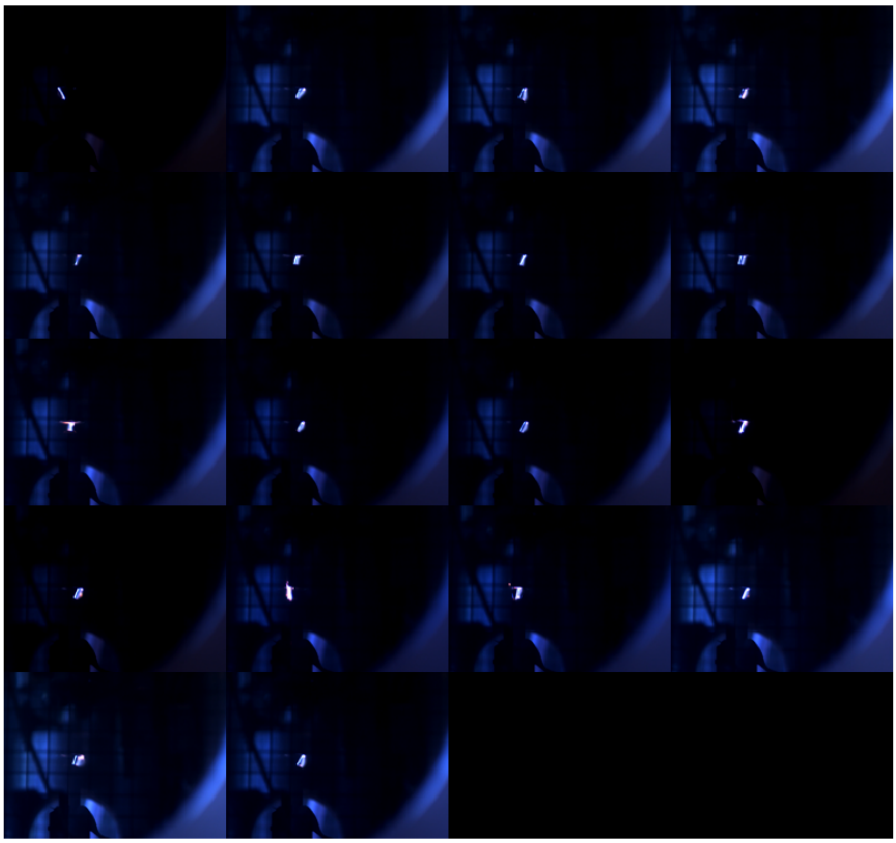

Figure 28: Air
Distance = 6 mm Pressure = 1.3 bar

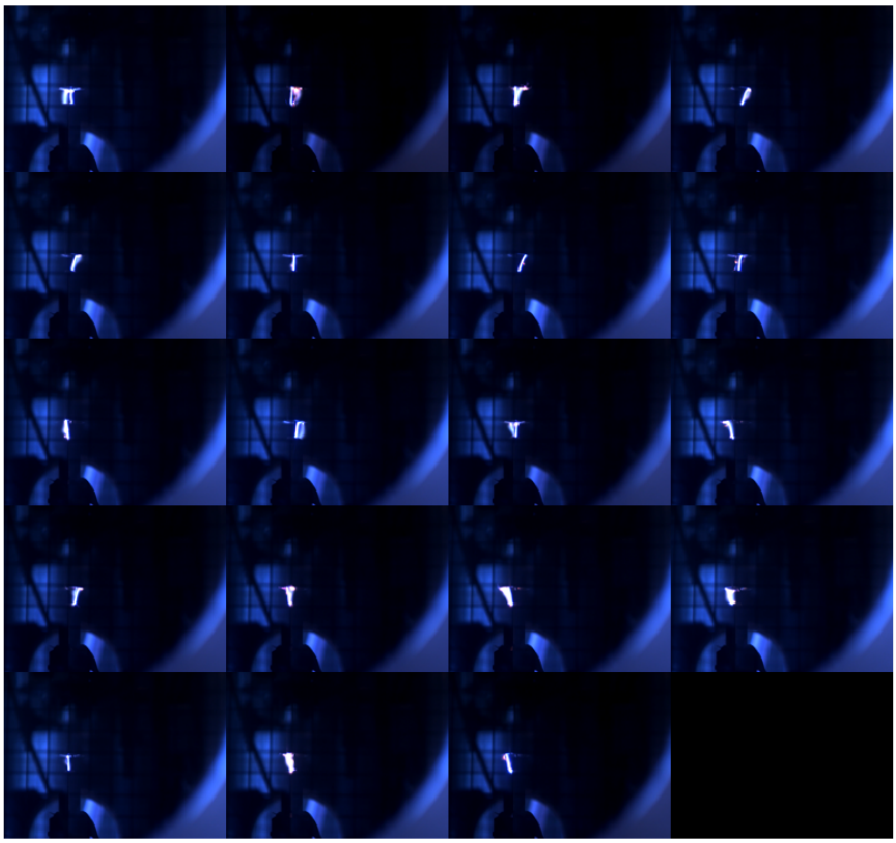

Figure 29: Air
Distance = 10 mm Pressure = 1.3 bar

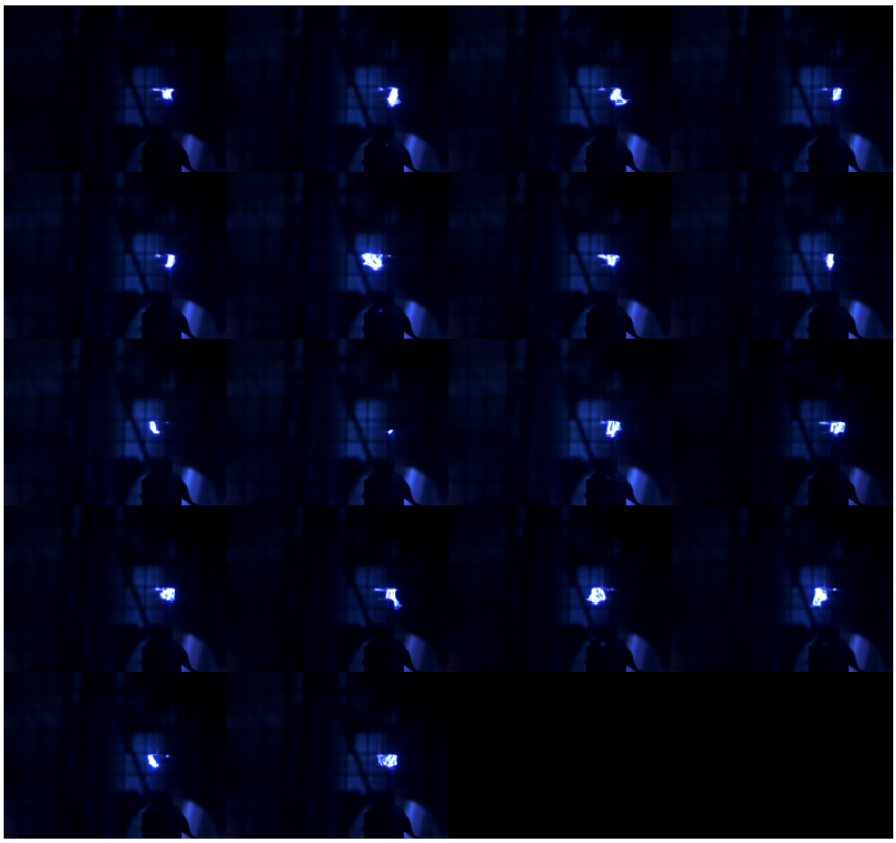

Figure 30: AirPlus
Distance = 6 mm Pressure = 1 bar

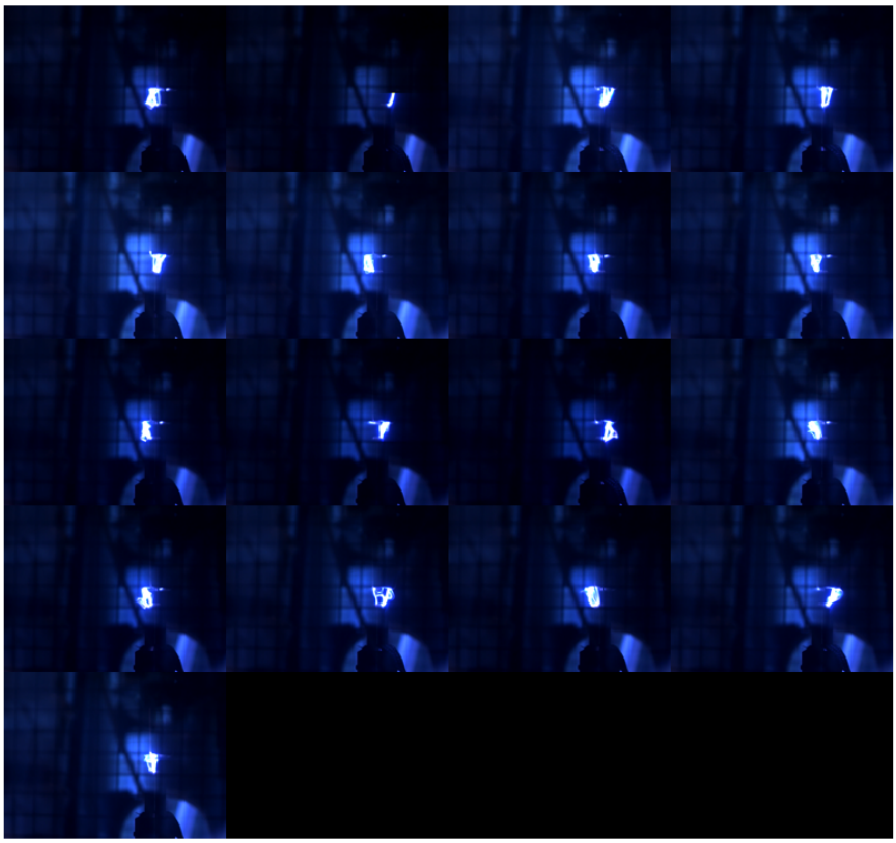

Figure 31: AirPlus
Distance = 10 mm Pressure = 1 bar

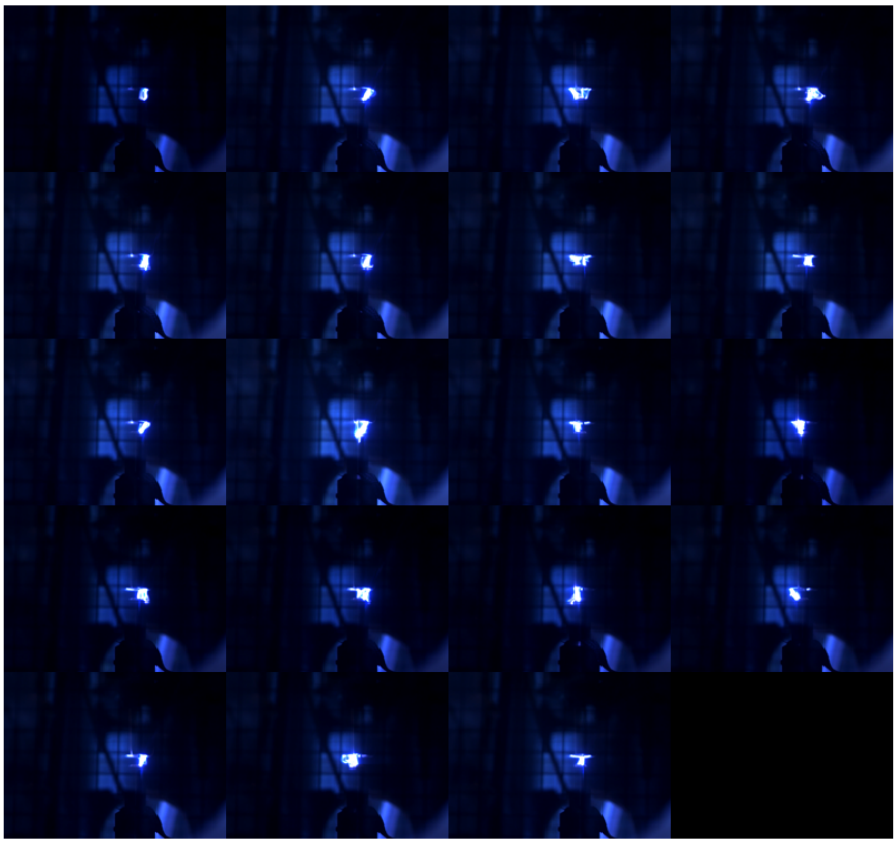

Figure 32: AirPlus
Distance = 6 mm Pressure = 1.3 bar

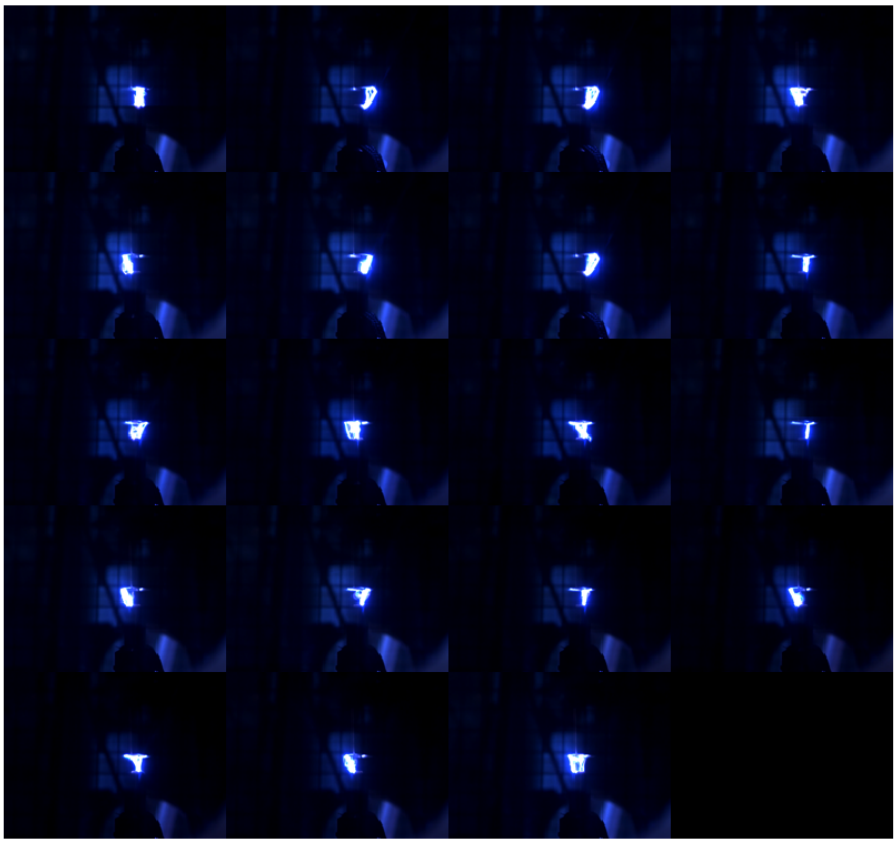

Figure 33: AirPlus
Distance = 10 mm Pressure = 1.3 bar

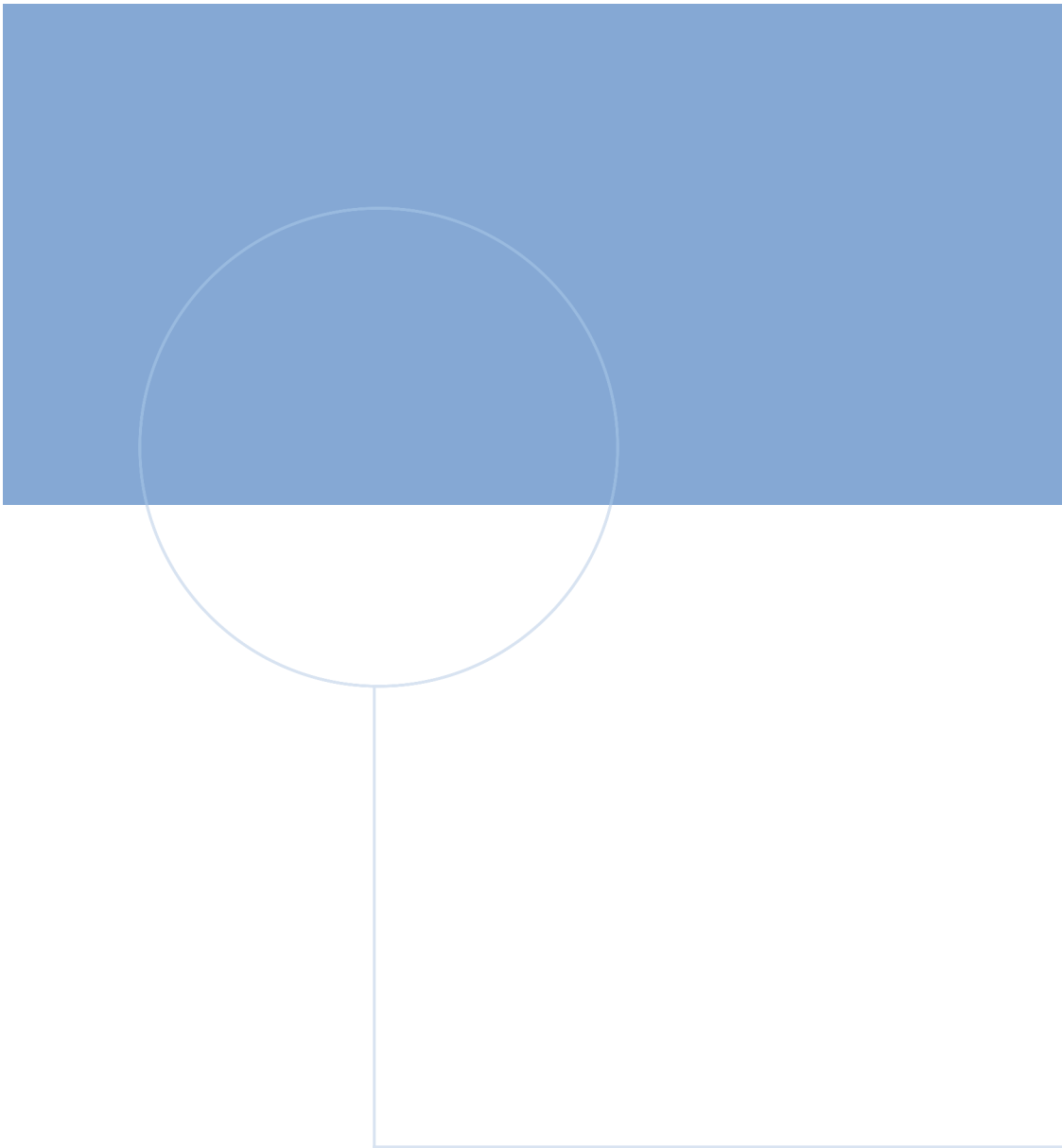

NTNU
Norwegian University of
Science and Technology